Three-dimensional Quantum Slit Diffraction and Diffraction in Time.

M. Beau & T. C. Dorlas
Dublin Institute for Advanced Studies
School of Theoretical Physics
10 Burlington Road, Dublin 4, Ireland.

February 17, 2014

Abstract

We study the quantum slit diffraction problem in three dimensions. In the treatment of diffraction of particles by a slit, it is usually assumed that the motion perpendicular to the slit is classical. Here we take into account the effect of the quantum nature of the motion perpendicular to the slit using the Green function approach [18]. We treat the diffraction of a Gaussian wave packet for general boundary conditions on the shutter. The difference between the standard and our three-dimensional slit diffraction models is analogous to the diffraction in time phenomenon introduced in [16]. We derive corrections to the standard formula for the diffraction pattern, and we point out situations in which this might be observable. In particular, we discuss the diffraction in space and time in the presence of gravity.

Contents

1 Introduction

The quantum slit diffraction experiment of electrons was first realized experimentally in 1961 by C. Jönsson, see [1] and [2], but the first experimental proof of the quantum diffraction for individual electrons was shown in the seventies by O. Donati, P. G. Merli, G. P. Missiroli and G. Pozzi, [3],[4] using electron biprisms and later independently by A. Tonomura, J. Endo, H. Ezawa, T. Matsuda and T. Kawasaki [5]. The quantum diffraction phenomenon has been interpreted via the famous thought experiment imagined by Richard Feynman in [6]. We mention that this double slit experiment has recently also been done experimentally [7] in a situation where the probability

distribution for individual electron on the screen was observed (statistically) while varying the position of a mask hiding one, two or none of the slits. In addition, nano-slit electron experiments were recently performed, see for example [8]. Furthermore, slit experiments were carried out with neutrons, see [9] and the references therein, ultracold atoms [10] and with heavy molecules such as C_{60}, see [11].

In [12], Feynman and Hibbs also treated in detail a quantum slit diffraction model using the path integral formalism to compute the quantum slit propagator. The model consists of a one-dimensional slit appearing in the motion of an electron at a time $\tau > t_0 = 0$ and then removed instantaneously, the electron striking the screen at a time $t > \tau$. Actually, this means that the motion of the electron from the source to the screen consists of two independent motions, the first from the source to the slit and the second from the slit to the screen. Under this hypothesis, the quantum propagator for the single-slit system can be written as a product of the free propagator in the x-direction orthogonal to the slit and the propagator along the one-dimensional slit axis z: see [13] and [14] for pedagogical presentations of this model. This so-called "*truncation assumption*" or "*truncation approximation*"[15] is convenient and valid under certain conditions. First, we suppose that the particle passes through the aperture at the classical time $\tau = t_c = D/v_x = (D/x)t$, where D is the distance between the emittor and the center of the slit, x is the distance between the emittor and the screen, and $v_x = x/t$ is the classical velocity related to the wave length λ by the de Broglie relation $\lambda \approx 2\pi\hbar/(mv_x) = 2\pi\hbar t/(mx)$. Here we assume $v \approx v_x$ because we have $a \ll x$, where a is the size of the slit, and we take $z \ll x$ where z is the position of the particle detected on the screen. This assumption means that the motion along the x-axis is classical whereas the one parallel to the screen (in the z direction) is quantum. The main goal of this article is to find the condition justifying the latter assumption, i.e. the classical behavior of the particle along the x-axis, independently of the fact that we consider the aperture of the slit to be relatively small, and also to obtain a correction to the single-slit propagator formula and to analyse the resulting effect on the probability density function for different regimes.

At this stage, we should mention that another curious quantum diffraction phenomenon was imagined in 1952 M. Moshinsky [16]. He showed that for a monochromatic plane wave moving along a one-dimensional line, if a perfectly absorbing screen is placed at a fixed position on the axis at the times $0 < t < t_1$ and is removed at the time t_1, the probability density function would be similar to the one observed for the diffraction in space by a half-plane. By analogy, therefore, we call this phenomenon *diffraction in time*. It was first observed experimentally in 1997 by the cold atom team of the Kastler Brossel

Institute in Paris, see [17]. In the mean time, the problem of diffraction in both space and time of monochromatic plane waves for a perfectly reflective slit-screen was treated in [18]. They used the Green's function method, giving the general solution of the diffusion equation [19] in the half-space delimited by the plane of the slit with given boundary conditions. Another approach was developed in [20] to construct the quantum propagator for a purely absorbing screen. Also, some recent progress have been made in [21] where an exactly solvable model of diffraction in time for a perfectly absorbing shutter was developed. There are other recent articles [22], [23] and review [24], on the diffraction in time phenomenon. Also we refer the reader to the series of articles dealing with diffraction in space and time for Gaussian wave packets [25], [26], [27] where the autor discusses the effect of the finite width of the wave packet.

In this article, we use the Brukner-Zeilinger approach [18] to construct the three-dimensional quantum slit propagator of a Gaussian wave packet for general boundary conditions on the slit (absorbing or reflective), and to derive a semi-classical formula for the propagator taking into account the diffraction in time. In Section II, we introduce the following model. Consider a particle, modeled by a three-dimensional Gaussian wave packet of width σ, which is emitted at the time $t_0 = 0$ from the position $x_0 < 0,\ y_0 = 0,\ z_0 = 0$. The aperture of the slit is closed until the time $t_1 \geq 0$ after which it is opened and the wave packet propagates from the rectangular aperture of the slit (centered at $x = 0$) to a screen (centered at $x > 0$) where the position (y, z) of the particle is detected at a time $t > t_1$. In Section III, we derive an explicit integral formula for the single-slit propagator (for a rectangular aperture) for arbitrary boundary conditions on the plane of the slit, in the case where the times of emission of the particle and of opening of the slit coincide: $t_1 = t_0 = 0$. After that, we will show that there is a *semi-classical transition*, when the parameter $\mu = m|\mathbf{r}|^2/(\hbar t)$ is large, where $\mathbf{r}$ is the position of the particle detected on the screen at the time t. We will also interpret the semi-classical propagator formula as a sum over classical paths going through the aperture at different times depending on the position at which the particle passes through the slit. To illustrate the semi-classical transition we calculate numerically the probability density function for a narrow Gaussian wave packet, $\sigma \sim 0$. In Section IV we give a correction to the truncation approximation propagator in the Fraunhofer regime when the dimensions of the aperture are small compared to the distance between the slit and the screen. Then we give a formula for the shift in the distance between two successive minima of the probability distribution function compared to the classical result. In the last section, we discuss an experimental perspective to the diffraction pattern for a relatively large aperture of the slit, particularly

for the slit diffraction experiment in the presence of a constant gravity field.

2 Diffraction in space (DIS) and in time (DIT) of a localized wave packet

The aim of this section is to recall the theory of diffraction in space and time and to give a general solution to the Schrödinger equation for an initial Gaussian wave packet on the half space delimited by a plane. The purpose of this study is to give the physical ingredients and the mathematical tools to treat the problem of the slit diffraction beyond the truncation approximation. The latter main problem will be explored in the subsequent sections.

2.1 Basic set up

The diffraction-in-time experiment consists of opening a shutter at position $x_1 = 0$ at a time $t_1 \geq 0$ and observing the particle at a point $x > 0$ after the opening time $t - t_1 > 0$. In [16] as well as in [18], the wave at the source is considered to be a monochromatic plane wave. Here we consider, as in [20], a localized wave packet (Gaussian), but we follow the method developed in [18] to find the general solution. To understand the difference between the localized wave packet versus plane wave, we notice that the phase of the wave is non-linear in space and in time (for one dimension $\varphi_t(x) = \frac{mx^2}{2\hbar t}$) and so the coordinate and time of emission of the localized wave has to be taken into account (which is not the case for a plane wave since the phase is linear in time, $\varphi_t(x) = kx - \frac{\hbar k^2 t}{2m}$). Thus, for the truncation approximation model, the half-plane diffraction amplitude for a Gaussian wave packet is given by Fresnel integrals (see [14]) whereas for a plane wave this amplitude is given by the Fourier transform of the shape of the aperture (for example of a two dimensional gate function for a rectangular aperture). We will see that the result for the space diffraction of a localized wave packet by an half-plane is actually similar to the so-called "diffraction in time".

To give a general solution of the diffraction in space and time problem, we first write the Schrödinger equation for the wave function of the particle moving in the apparatus:

$$\begin{array}{l} \frac{\hbar^2}{2m}\nabla^2\psi(\mathbf{r},t) + i\hbar\frac{\partial}{\partial t}\psi(\mathbf{r},t) = 0 \\ \psi(\mathbf{r},t) = 0 \text{ for } x > x_1 \text{ and } t < t_1, \text{ and } \psi(\mathbf{r}_1,t) = \phi(\mathbf{r}_1,t) \text{ for } t > t_1. \end{array} \quad (1)$$

Here we fixed the initial condition in the half-plane to be zero at times $t < t_1$ and inhomogeneous Dirichlet boundary conditions on the plane of

the slit $x = x_1$ for $t > t_1$. In [18], the boundary condition is taken to be a monochromatic plane wave $\phi(\mathbf{r}_1, t) = e^{-i\omega_0 t}$, whereas here we will consider a localized wave packet (Gaussian).

We would like to write the solution of (1) using the point source method by computing the Green function solution of the equation:[19]

$$\frac{\hbar^2}{2m}\nabla^2 G(\mathbf{r}, t, \mathbf{r}', \tau) + i\hbar\frac{\partial G(\mathbf{r}, t, \mathbf{r}', \tau)}{\partial t} = i\hbar\delta^3(\mathbf{r} - \mathbf{r}')\delta(t - \tau) \tag{2}$$

with the causality conditions:

$$G(\mathbf{r}, t < \tau, \mathbf{r}', \tau) = 0,\ \nabla G(\mathbf{r}, t < \tau, \mathbf{r}', \tau) = 0 \tag{3}$$

The free Green function for infinite volume with the conditions (3) is:

$$G_0(\mathbf{r} - \mathbf{r}'; t - \tau) = \left(\frac{m}{2i\pi\hbar(t - \tau)}\right)^{3/2} e^{\frac{im|\mathbf{r}-\mathbf{r}'|^2}{2\hbar(t-\tau)}}\theta(t - \tau) \tag{4}$$

Here we recall the solution of the Schrödinger equation (1) and we refer the reader to [18] and [19] for more details:

$$\begin{aligned}\psi(\mathbf{r}, t) &= \int_V d^3\mathbf{r}' G(\mathbf{r}, t, \mathbf{r}^{'}, t_1)\psi(\mathbf{r}^{'}, t_1) \\ &+ \frac{i\hbar}{2m}\int_{t_1}^{t} d\tau \int_{\partial V} d\mathbf{S}_1 \left[G(\mathbf{r}, t, \mathbf{r}_1, \tau)\nabla_{\mathbf{r}_1}\psi(\mathbf{r}_1, \tau) - \psi(\mathbf{r}_1, \tau)\nabla_{\mathbf{r}_1} G(\mathbf{r}, t, \mathbf{r}_1, \tau)\right]\end{aligned} \tag{5}$$

Here ∂V is the boundary of the half-plane, i.e. the 2-dimensional surface $x = x_1$.

In the following, we denote by $\mathbf{r}_\perp = (y, z)$ the coordinates in the plane orthogonal to the x-axis and $\mathbf{r}_{\perp,1} = (y_1, z_1)$ the same at the shutter. We consider general homogeneous conditions for the Green function:

$$G(\mathbf{r}, t, \mathbf{r}_1, \tau) = \lambda_1 G_0(x - x_1, \mathbf{r}_\perp - \mathbf{r}_{\perp,1}; t - \tau) + \lambda_2 G_0(x + x_1, \mathbf{r}_\perp - \mathbf{r}_{\perp,1}; t - \tau)\ . \tag{6}$$

By a direct calculus we have :

$$\partial_{x_1} G(\mathbf{r}, t, \mathbf{r}_1, t_1)|_{x_1=0} = (-\lambda_1 + \lambda_2)\frac{im}{\hbar}\frac{x}{t - \tau}G_0(x, \mathbf{r}_\perp - \mathbf{r}_{\perp,1}; t - t_1) \tag{7}$$

In particular we have the following special cases:
(i) for $\lambda_1 = 1\,\lambda_2 = -1$, we have the homogeneous Dirichlet conditions, $G(\mathbf{r}, t, \mathbf{r}_1, \tau)|_{x_1=0} = 0$
(ii) for $\lambda_1 = 1\,\lambda_2 = 1$, we get the homogeneous Neumann conditions,

$\partial_{x_1} G(\mathbf{r}, t, \mathbf{r}_1, \tau)|_{x_1=0} = 0$
(iii) for $\lambda_1 = 1\,\lambda_2 = 0$, we get the free Green's function $G(\mathbf{r}, t, \mathbf{r}_1, \tau) = G_0(\mathbf{r} - \mathbf{r}_1; t - \tau)$

Notice that the volume is the half-space to the right-hand side of the shutter $V = [0, +\infty) \times \mathbb{R} \times \mathbb{R}$ and we consider that the initial wave function vanishes in this domain $\psi(\mathbf{r}', t_1) = 0$, if $x' > 0$, with $\mathbf{r}' = (x', y', z')$. Then by (5), we get the following solution :

$$\psi(\mathbf{r}, t) = \frac{i\hbar}{2m} \int_{t_1}^{t} d\tau \int_{\partial V} d\mathbf{S}_1 \left[G(\mathbf{r}, t, \mathbf{r}_1, \tau) \nabla_{\mathbf{r}_1} \psi(\mathbf{r}_1, \tau) - \psi(\mathbf{r}_1, \tau) \nabla_{\mathbf{r}_1} G(\mathbf{r}, t, \mathbf{r}_1, \tau) \right]_{x_1=0} . \tag{8}$$

Note that $d\mathbf{S}_1$ is the elementary boundary surface vector orthogonal to the plane at the point $\mathbf{r}_1$ and pointing outward of the volume (i.e. $d\mathbf{S}_1 = -dy_1 dz_1 \mathbf{e}_x$). On the surface of the aperture ∂V, we consider that after opening the shutter, the wave function is a Gaussian wave packet which was emitted at time $t_0 = 0$, and therefore given by the following wave function at each point $\mathbf{r}_1 \in \partial V$:

$$\psi(\mathbf{r}_1, \tau) = \int_{\mathbb{R}^3} d\mathbf{R}\; G_0(\mathbf{r}_1 - \mathbf{R}; \tau) \phi(\mathbf{R}, 0) \theta(\tau - t_1) \;, \tag{9}$$

where the normalized Gaussian wave packet ϕ is given by:

$$\phi(\mathbf{R}, 0) = \frac{1}{(2\pi\sigma^2)^{3/4}} e^{-\frac{|\mathbf{R}-\mathbf{r}_0|^2}{4\sigma^2}} \;, \tag{10}$$

where $\mathbf{R} = (X, Y, Z)$ and so X denotes the coordinate along the x-axis. The probability density for the initial wave packet is such that $|\phi(\mathbf{R}, 0)|^2 \to \delta^3(\mathbf{R} - \mathbf{r}')$ when $\sigma \to 0$. In the sequel we will consider the case that σ is small compared to the distance $|x_1 - x_0|$ between the position x_0 of the center of the Gaussian of the wave packet and the position of the shutter x_1.

Remark. To relate the conditions (9) to the condition in [18], let us rewrite the initial condition at the emission of the wave packet as a Gaussian distribution of plane waves:

$$\phi(\mathbf{R}, 0) = \int_{\mathbb{R}^3} d\mathbf{k}\; \varphi_{\mathbf{k}}(\mathbf{r}_0 - \mathbf{R}, 0) e^{-\frac{\sigma^2}{2}\mathbf{k}^2} \tag{11}$$

where $\phi_{\mathbf{k}}(\mathbf{r}_0 - \mathbf{R}, 0) = e^{i\mathbf{k}\cdot(\mathbf{r}_0 - \mathbf{R})}$. Then, if we choose the same boundary condition on the surface $(x_1 = 0, y_1, z_1)$ for the plane waves defined just above as the one considered in [18]:

$$\varphi_{\mathbf{k}}(\mathbf{r}_0 - \mathbf{R}, \tau) = e^{i\mathbf{k}\cdot(\mathbf{r}_1 - \mathbf{r}_0)} e^{-i\omega\tau} \theta(\tau - t_1) \tag{12}$$

with the dispersion relation $\omega = \frac{\hbar \mathbf{k}^2}{2m}$, we directly get (9) from (12) and (11). Notice that in (10) we have arbitrarily chosen the initial wave vector to be zero, but we could generally set:

$$\phi_{\mathbf{k}_0}(\mathbf{R}, 0) = \frac{1}{(2\pi\sigma^2)^{3/4}} e^{-\frac{|\mathbf{R}-\mathbf{r}_0|^2}{4\sigma^2}} e^{i\mathbf{k}_0 \cdot (\mathbf{r}_0 - \mathbf{R})} \ , \tag{13}$$

where the initial wave vector is $\mathbf{k}_0$. However, in the following, we will assume that σ is close to zero and so there will not be a privileged initial wave vector, which is why we take $\mathbf{k}_0 = \mathbf{0}$ in the sequel.

By (8) and (9), we get the following formula

$$\psi(\mathbf{r}, t) = \int_{R^3} d\mathbf{R} \ K(\mathbf{r}, t, \mathbf{R}, 0 | \partial V, t_0) \phi(\mathbf{R}, 0) \tag{14}$$

where the propagator is defined by:

$$K(\mathbf{r}, t, \mathbf{R}, 0 | \partial V, t_1) \equiv$$
$$\frac{i\hbar}{2m} \int_{t_1}^{t} d\tau \int_{\partial V} d\mathbf{S}_1 \cdot [G(\mathbf{r}, t, \mathbf{r}_1, \tau) \nabla_{\mathbf{r}_1} G_0(\mathbf{r}_1 - \mathbf{R}, \tau) - G_0(\mathbf{r}_1 - \mathbf{R}, \tau) \nabla_{\mathbf{r}_1} G(\mathbf{r}, t, \mathbf{r}_1, \tau)]_{x_1 = 0} \tag{15}$$

Remark. To avoid confusion, we stress that (14) is different from the volume integral term of the general solution (5): we have just rewritten (8) using the expression (15) and the integral (9).

Since

$$\nabla_{\mathbf{r}_1} G_0(\mathbf{r}_1 - \mathbf{R}, \tau) = \frac{im}{\hbar} \frac{\mathbf{r}_1 - \mathbf{R}}{\tau} G_0(\mathbf{r}_1 - \mathbf{R}, \tau)$$
$$\nabla_{\mathbf{r}_1} G(\mathbf{r}, t, \mathbf{r}_1, \tau) = \frac{im}{\hbar} \left(-\lambda_1 \frac{\mathbf{r} - \mathbf{r}_1}{t - \tau} + \lambda_2 \frac{\mathbf{r} + \mathbf{r}_1}{t - \tau} \right) G_0(\mathbf{r} - \mathbf{r}_1, \tau)$$

we get:

$$K(\mathbf{r}, t, \mathbf{R}, 0 | \partial V, t_1) = -\frac{1}{2} \int_{t_1}^{t} d\tau \int_{\partial V} d\mathbf{S}_1 \cdot \Big($$
$$\left[\frac{\mathbf{r}_1 - \mathbf{R}}{\tau} (\lambda_1 + \lambda_2) + \lambda_1 \frac{\mathbf{r} - \mathbf{r}_1}{t - \tau} - \lambda_2 \frac{\mathbf{r} + \mathbf{r}_1}{t - \tau} \right]_{x_1 = 0} G_0(\mathbf{r} - \mathbf{r}_1, t - \tau) G_0(\mathbf{r}_1 - \mathbf{R}, \tau)|_{x_1 = 0} \Big) \tag{16}$$

2.2 One-dimensional diffraction in time of a localized wave packet

Consider the one-dimensional diffraction-in-time problem for a Gaussian wave packet emitted at $x_0 < 0$ at the time 0. By similar arguments to those leading to (16), we get, for general boundary conditions, the following propagator:

$$K(x,t,X,0|x_1=0,t_1) = \int_{t_1}^{t} d\tau \left[\frac{-X}{\tau}\eta_1 + \frac{x}{t-\tau}\eta_2\right] G_0(x,t-\tau)G_0(-X,\tau) \tag{17}$$

where we put

$$\eta_1 = \frac{1}{2}\left(\lambda_1 + \lambda_2\right) \tag{18}$$

$$\eta_2 = \frac{1}{2}\left(\lambda_1 - \lambda_2\right). \tag{19}$$

Notice that choosing $\eta \equiv \eta_2 = 1 - \eta_1$, $\eta \in \mathbb{C}$ and taking $t_1 = 0$, a direct calculation shows that the integral in (17) is equal to $G_0(x - X; t)$ and so it gives the general solution for the free particle motion, see [20]. Now, if we take $\eta = 1/2$ (i.e. $\lambda_2 = 0$ and $\lambda_1 = 1$) then we get the free boundary condition corresponding to the perfectly absorbing shutter-screen condition. The correct solution for $t_1 > 0$ is equivalent to the Moshinsky solution:

$$K^{(0)}(x,t,X,0|x_1=0,t_1) = \frac{1}{2}\int_{t_1}^{t} d\tau \ \left[-\frac{X}{\tau} + \frac{x}{t-\tau}\right] G_0(x,t-\tau)G_0(-X,\tau) \tag{20}$$

which is easily evaluated (see [20]):

$$K^{(0)}(x,t,X,0|x_1=0,t_1) = \\ G_0(x-X;t)\left(1 + \frac{1}{2}\mathrm{erfc}\left(\left(x\frac{t_1}{t} + X\frac{t-t_1}{t}\right)\left(\frac{mt}{2i\hbar t_1(t-t_1)}\right)^{1/2}\right)\right) \tag{21}$$

Hence, by (17), we get the propagator for general homogeneous boundary conditions,

$$K^{(G)}(x,t,X,0|x_1=0,t_1) = \lambda_1 K^{(0)}(x,t,X,0|x_1=0,t_1) - \lambda_2 K^{(0)}(x,t,-X,0;x_1=0,t_1)\,. \tag{22}$$

similar to the case of a monochromatic plane wave [18]. For $\lambda_1 = -\lambda_2 = +1$ we get Dirichlet boundary conditions whereas for $\lambda_1 = \lambda_2 = +1$ we have Neumann boundary conditions.

The solution of the one-dimensional Schrödinger equation for the perfectly absorbing shutter-screen is obtained by inserting (20) into the one-dimensional version of (14):

$$\psi(x,t) = \int_{-\infty}^{+\infty} dX\ K^{(0)}(x,t;X,0|x_1=0,t_1)\psi(X,0)$$
$$= \int_{-\infty}^{+\infty} dX\ K^{(0)}(x,t;X,0|x_1=0,t_1)\frac{e^{-\frac{(X-x_0)^2}{4\sigma^2}}}{(2\pi\sigma^2)^{1/4}}. \quad (23)$$

In particular, if we assume that $\sigma \ll |x_0|$, we get that $\psi(x,t) \approx (8\pi\sigma)^{1/4}K^{(0)}(x,t;x_0,0|x_1 = 0,t_1)$.

Notice that the explicit solution (21) for $\sigma \ll |x_0|$ is similar to the explicit formulas giving the propagator and the wave function for the half-plane diffraction problem in the truncation approximation [20]. So both diffraction phenomena are analogous and this is why we use the term "diffraction in time" even for the localized wave packet. In the next subsection, we will see that we can also construct an analogous Moshinsky shutter problem for a localized wave packet and show the equivalence between both approaches for general homogeneous boundary conditions.

3 One-slit diffraction model and its semi-classical approximation

In the last section, we gave the theory of diffraction in space and time for a wave packet and we furnished the general solution of the Schrödinger equation for an initial Gaussian wave packet passing through an aperture which is opened at a time $t_1 \geq t_0 = 0$, where t_0 is the time of the emission of the initial wave packet. We have also seen that we can interpret this phenomenon as a diffraction in time by analogy with the diffraction in space. However, since the main problem of this article is to derive a formula for the slit diffraction problem, where the aperture is not assumed to be small compared with the distance between the slit and the screen (and the slit and the source), we would like to interpret the so-called diffraction in time phenomenon in a different way, where the apparatus is fixed in time (no shutter) and the problem is stationary. In this section, we apply the theory developed in the previous section to the slit diffraction problem and give a geometric interpretation for the propagator. We first give an explicit formula for the propagator with general boundary conditions, then give its semi-classical expression and comment on the results. We also give numerical results for

intensity patterns on the screen in the delta limit $\sigma \to 0$ for the Dirichlet, Neumann and free boundary conditions and comment on the differences. In the next section, we will use the semi-classical formula of the propagator to give corrections to the truncation approximation model.

3.1 Single-slit diffraction of a narrow Gaussian wave packet

We consider the slit $\Omega_{a,b} \equiv \{x_1 = 0\} \times [-b, b] \times [-a, a]$, and assume that the shutter is open at the time $t_1 = 0$. The dynamics of the particle obeys the Schrödinger equation (1) and the boundary conditions are given by (9), (10). Here we consider the general homogeneous boundary conditions (6). By (16) we get the following formula for the propagator:

$$K^{(a,b)}(\mathbf{r}, t, \mathbf{R}, 0) = \int_0^t d\tau \int_{-a}^{a} dz_1 \int_{-b}^{b} dy_1 \left[\frac{-X}{\tau}\eta_1 + \frac{x}{t-\tau}\eta_2 \right] G_0(\mathbf{r}-\mathbf{r}_1, t-\tau) G_0(\mathbf{r}_1-\mathbf{R}, \tau) \tag{24}$$

The integral over the time of the one-point source propagator (for every $\mathbf{r}_1 \in \partial V$ fixed) can be evaluated explicitly. The resulting formula will be analyzed in the semi-classical limit using the stationary phase approximation method which yields a semi-classical interpretation of the propagator. The one-slit propagator is then given by an integral of this one-point source propagator over the aperture of the slit. Finally, the wave function on the screen at time t is given by (14), where we consider an initial narrow Gaussian wave packet (10) of width σ which is small compared to the distance between the center of the Gaussian and the slit and also to the size of the aperture:

$$\sigma \ll |\mathbf{r}_0|,\ a, b.$$

By (14) we then have the following approximation:

$$\begin{aligned} \psi(\mathbf{r}, t) &= (8\pi\sigma^2)^{3/4} \int_{R^3} d\mathbf{R}\ K^{(a,b)}(\mathbf{r}, t, \mathbf{R}, 0) \frac{e^{-\frac{|\mathbf{R}-\mathbf{r}_0|^2}{4\sigma^2}}}{(2\pi\sigma^2)^{3/2}} \\ &\approx (8\pi\sigma^2)^{3/4} K^{(a,b)}(\mathbf{r}, t, \mathbf{r}_0, 0),\ \text{when } \sigma \sim 0 \end{aligned} \tag{25}$$

Therefore, in the sequel we will take $\mathbf{R} = \mathbf{r}_0$ in (24) since the final wave function is just proportional to the one-slit propagator.

Remark. In the limit $\sigma \to 0$, we would like to give a formula for the probability density for the particle to be at the point $\mathbf{r}$ on the screen at the time t. This has already been done for the truncation approximation, see

[14] and Appendix 1, and the general idea here is similar. It is important to realize that $|\psi(\mathbf{r},t)|^2$ represents the non-normalized wave function at the point $\mathbf{r}$ on the screen at the time t and so, to get the probability, we have to divide by the total mass on the screen:

$$M \equiv \int_{-\infty}^{+\infty} dy \int_{-\infty}^{+\infty} dz \ |\psi(\mathbf{r},t)|^2 \ .$$

For the truncation approximation model, the particle is assumed to pass through the slit at the classical time t_c (given by a linear relation between t and the distances along the x-axis). Hence, the total mass passing to the right side of the plane of the slit is equal to the total mass on the screen:

$$\int_{-b}^{b} dy_1 \int_{-a}^{a} dz_1 \ |\psi_{\text{Trunc}}(\mathbf{r}_1,t_c)|^2 = \int_{-\infty}^{+\infty} dy \int_{-\infty}^{+\infty} dz \ |\psi_{\text{Trunc}}(\mathbf{r},t)|^2 \qquad (26)$$

However, in our model there is no similar conservation equation to (26) since we do not know the exact time when the particle passes through the aperture. Hence, the expression for the probability density at the point $\mathbf{r}$ and at the time t has to written as

$$P(\mathbf{r},t) = \frac{1}{M}|\psi(\mathbf{r},t)|^2 \to \frac{1}{\Omega}|K^{(a,b)}(\mathbf{r},t,\mathbf{r}_0,0)|^2, \text{ when } \sigma \to 0 \qquad (27)$$

where $\Omega \equiv \int_{-\infty}^{+\infty} dy \int_{-\infty}^{+\infty} dz |K^{(a,b)}(\mathbf{r},t,\mathbf{r}_0,0)|^2$.

The formula (24) can be rewritten as an integral over all points $\mathbf{r}_1 = (x_1,y_1,z_1)$ in the slit (i.e. $y_1 \in [-b,b]$ and $z_1 \in [-a,a]$):

$$K^{(a,b)}(\mathbf{r},t,\mathbf{r}_0,0) = \int_{-a}^{a} dz_1 \int_{-b}^{b} dy_1 K(\mathbf{r},t;\mathbf{r}_0,0|\mathbf{r}_1) \ , \qquad (28)$$

where we have defined the three-dimensional one-point source propagator:

$$K(\mathbf{r},t;\mathbf{r}_0,0|\mathbf{r}_1) \equiv \int_0^t d\tau \left[\frac{-x_0}{\tau}\eta_1 + \frac{x}{t-\tau}\eta_2\right] G_0(\mathbf{r}-\mathbf{r}_1,t-\tau)G_0(\mathbf{r}_1-\mathbf{r}_0,\tau) \ . \qquad (29)$$

We want to give an explicit formula for the one-point slit propagator (29). For a detailed calculuation we refer the reader to Appendix 2. The result is the following explicit formula:

$$K(\mathbf{r},t;\mathbf{r}_0,0|\mathbf{r}_1) = A_t(\mathbf{r};\mathbf{r}_0|\mathbf{r}_1)e^{i\varphi_t(\mathbf{r};\mathbf{r}_0|\mathbf{r}_1)} \qquad (30)$$

where the phase is given by

$$\varphi_t(\mathbf{r},\mathbf{r}_0|\mathbf{r}_1) \equiv \frac{m}{2\hbar t}(|\mathbf{r}-\mathbf{r}_1| + |\mathbf{r}_1-\mathbf{r}_0|)^2 \qquad (31)$$

and where the amplitude is given by a linear combination of the Neumann and Dirichlet amplitudes:

$$A_t(\mathbf{r}, \mathbf{r}_1 - \mathbf{r}_0) \equiv \eta_1 A_t^{(N)}(\mathbf{r}, \mathbf{r}_1 - \mathbf{r}_0) + \eta_2 A_t^{(D)}(\mathbf{r}, \mathbf{r}_1 - \mathbf{r}_0). \tag{32}$$

The Neumann part is given by:

$$A_t^{(N)}(\mathbf{r}, \mathbf{r}_0|\mathbf{r}_1) = \frac{-x_0}{(2i\pi\hbar t/m)^{3/2}} \left(\frac{m}{2i\pi\hbar t} \frac{(|\mathbf{r} - \mathbf{r}_1| + |\mathbf{r}_1 - \mathbf{r}_0|)^2}{|\mathbf{r} - \mathbf{r}_1||\mathbf{r}_1 - \mathbf{r}_0|^2} + \frac{1}{2\pi|\mathbf{r}_1 - \mathbf{r}_0|^3} \right) \tag{33}$$

and the Dirichlet part by:

$$A_t^{(D)}(\mathbf{r}, \mathbf{r}_0|\mathbf{r}_1) = \frac{x}{(2i\pi\hbar t/m)^{3/2}} \left(\frac{m}{2i\pi\hbar t} \frac{(|\mathbf{r} - \mathbf{r}_1| + |\mathbf{r}_1 - \mathbf{r}_0|)^2}{|\mathbf{r} - \mathbf{r}_1|^2|\mathbf{r}_1 - \mathbf{r}_0|} + \frac{1}{2\pi|\mathbf{r} - \mathbf{r}_1|^3} \right). \tag{34}$$

Remark. The equation (28) gives the correct propagator formula for the slit diffraction problem, whatever the initial condition for the wave at $t_0 = 0$. For example, we can take the following more general condition than (13):

$$\phi_{\mathbf{k}_0}(\mathbf{R} = (X, Y, Z), 0) = \frac{1}{((2\pi)^3\sigma_x^2\sigma_y^2\sigma_z^2)^{1/4}} e^{-\frac{|X-x_0|^2}{4\sigma_x^2}} e^{-\frac{|Y-y_0|^2}{4\sigma_y^2}} e^{-\frac{|Z-z_0|^2}{4\sigma_z^2}} e^{i\mathbf{k}_0\cdot(\mathbf{r}_0-\mathbf{R})},$$

where σ_y, σ_z are small but σ_x is large, and consider in the limit delta-distributions along the y- and z-axis and a plane wave along the x-axis. Then, the approximation we made for $\sigma \sim 0$ is still valid in the plane of the slit but not on the x-axis which can be considered the *propagation axis*. In this limit, to get the wave solution, we have to compute the Fourier transform of (28) with respect to x_0:

$$\psi(\mathbf{r}, t) \approx \left(32\pi \frac{\sigma_y^2\sigma_z^2}{\sigma_x^2} \right)^{1/4} \int_{-\infty}^{+\infty} dx_0 \; K^{(a,b)}(\mathbf{r}, t, \mathbf{R}, 0) \; e^{ik_{0,x}x_0}$$

3.2 Semiclassical limit of the one-slit propagator

In the following we still assume that the opening of the aperture of the slit coincides with the emission of the Gaussian wave packet $t_1 = t_0 = 0$, and that the width of the Gaussian is small compared to the distances of the apparatus, $\sigma \ll |x_0|, a, b$, so that (25) gives a good approximation to the solution.

Now we will give the semi-classical approximation of the propagator (28) when the fluctuation of the phase tends to zero, i.e. considering that $\mu \equiv \frac{m|\mathbf{r}|^2}{\hbar t} \gg 1$ and so that $|\mathbf{r}| \gg \lambda_0$ with $\lambda_0 \equiv \sqrt{2\pi\hbar t/m}$. This allows us to

interpret the propagator of the slit experiment in this regime as the sum over classical paths starting from $\mathbf{r}_0$ at the time $t_0 = 0$ to $\mathbf{r}$ at the time t given that the particle passes through the slit $\mathbf{r}_1 \in \Omega_{a,b}$ at a so-called *semi-classical time* $\tau_{sc} \in (0, t)$. The results are similar to the ones obtained for the truncation approximation model (see [14] and Appendix 1) but not the same since we do not make any geometrical approximation and, as a consequence, τ_{sc} depends on the coordinates $\mathbf{r}_1$ of the classical paths passing through the slit. We should mention that another condition for the validity of the semi-classical approximation is that the distances $|\mathbf{r} - \mathbf{r}_1|$ and $|\mathbf{r}_1 - \mathbf{r}_0|$ have to be of the same order for every $(y_1, z_1) \in \Omega_{a,b}$, which means that $|x_0|$ and $|x|$ are also of the same order, and that the sizes of the aperture $a,\ b$ and the position of the screen $|y|,\ |z|$ have to be at most of the same order as $|x|$.

By the above assumptions, we are able to use the stationary phase approximation applied to the one-point propagator formula(29):

$$\int_0^t d\tau f(\tau) e^{i\mu\phi(\tau)} \approx f(\tau_{sc}) e^{i\mu\phi(\tau_{sc})} \int_0^t d\tau\ e^{\frac{i\mu}{2}\phi''(\tau_{sc})(\tau-\tau_{sc})^2},\ \mu \gg 1 \tag{35}$$

where τ_{sc} is the solution of the equation $\phi'(\tau) = 0$, $\phi''(\tau_{sc})$ is the second derivative of ϕ at the point τ_{sc}, and where we put

$$\begin{array}{l} f(\tau) = \frac{1}{((2i\pi\hbar/m)^2(t-\tau)\tau)^{3/2}} \left(\frac{-x_0}{\tau}\eta_1 + \frac{x}{(t-\tau)}\eta_2\right) \\ \mu = \frac{m|\mathbf{r}|^2}{2\hbar t} = \frac{\pi|\mathbf{r}|^2}{\lambda_0^2} \\ \phi(\tau) = \frac{|\mathbf{r}-\mathbf{r}_1|^2}{|\mathbf{r}|^2(1-\tau/t)} + \frac{|\mathbf{r}_1-\mathbf{r}_0|^2}{|\mathbf{r}|^2\tau/t} \end{array} \tag{36}$$

By a direct calculation, we find that the saddle point τ_{sc} which is the solution of the equation $\phi'(\tau) = 0$ is given by

$$\tau_{sc} = \frac{|\mathbf{r}_1 - \mathbf{r}_0|}{|\mathbf{r} - \mathbf{r}_1| + |\mathbf{r}_1 - \mathbf{r}_0|} t \tag{37}$$

Then we get:

$$\begin{array}{l} f(\tau_{sc}) = \frac{1}{((2i\pi\hbar/m)^2(t-\tau_{sc})\tau_{sc})^{3/2}} \left(\frac{-x_0}{\tau_{sc}}\eta_1 + \frac{x}{(t-\tau_{sc})}\eta_2\right) \\ \mu\phi(\tau_{sc}) = \frac{m|\mathbf{r}-\mathbf{r}_1|^2}{2\hbar(t-\tau_{sc})} + \frac{m|\mathbf{r}_1-\mathbf{r}_0|^2}{2\hbar\tau_{sc}} = \frac{m}{2\hbar t}\left(|\mathbf{r} - \mathbf{r}_1| + |\mathbf{r}_1 - \mathbf{r}_0|\right)^2 \\ \mu\phi''(\tau_{sc}) = \frac{m}{\hbar}\left(\frac{|\mathbf{r}-\mathbf{r}_1|^2}{(t-\tau_{sc})^3} + \frac{|\mathbf{r}_1-\mathbf{r}_0|^2}{\tau_{sc}^3}\right) = \frac{m}{\hbar}\frac{t^3}{(t-\tau_{sc})^3\tau_{sc}^3}\frac{|\mathbf{r}-\mathbf{r}_1|^2|\mathbf{r}_1-\mathbf{r}_0|^2}{(|\mathbf{r}-\mathbf{r}_1|+|\mathbf{r}_1-\mathbf{r}_0|)^2} \end{array} \tag{38}$$

To estimate the integral at the right hand side of (35), we need to integrate in the complex plane along a contour, which we take to be the perimeter of

the eighth part of a circle centered at $-\tau_{sc}$ on the real axis and of radius t, together with the radii. Putting $N \equiv \mu\phi''(\tau_{sc})$, we get the following estimate for large N:

$$\int_{-\tau_{sc}}^{t-\tau_{sc}} ds\, e^{i\frac{Ns^2}{2}} = e^{i\frac{\pi}{4}} \int_{-\tau_{sc}}^{t-\tau_{sc}} ds\, e^{-\frac{Ns^2}{2}} + it \int_0^{\frac{\pi}{4}} d\theta\, e^{i\theta} e^{-\frac{Nt^2}{2}e^{2i\theta}} = (\frac{2i\pi}{N})^{1/2} + O(\frac{1}{N})\,, \tag{39}$$

since the latter integral is of the order $1/N$.

Hence by (35) and (39), we get the following approximation for the one-point propagator:

$$\begin{aligned} K_t(\mathbf{r}, \mathbf{r}_0|\mathbf{r}_1) &\approx f(\tau_{sc}) \left(\frac{2i\pi}{\mu\phi''(\tau_{sc})}\right)^{1/2} e^{i\mu\phi(\tau_{sc})} \\ &= \frac{(|\mathbf{r}-\mathbf{r}_1| + |\mathbf{r}_1-\mathbf{r}_0|)^2}{(2i\pi\hbar t/m)^{5/2}|\mathbf{r}-\mathbf{r}_1| \times |\mathbf{r}_1-\mathbf{r}_0|} \left(\frac{-x_0}{|\mathbf{r}_1-\mathbf{r}_0|}\eta_1 + \frac{x}{|\mathbf{r}-\mathbf{r}_1|}\eta_2\right) e^{\frac{im}{2\hbar t}(|\mathbf{r}-\mathbf{r}_1|+|\mathbf{r}_1-\mathbf{r}_0|)^2}\,. \end{aligned} \tag{40}$$

The stationary phase approximation method, leading to the formula (40), thus yields the propagator (30) except for the last terms of (34) and (33). Indeed, the phase is the same and the amplitude is a linear combination of the first term of the amplitudes (34), (33). We can explain this result remarking that both first terms in (34) and (33) are large compared to the second terms since the ratio is of the order $m|\mathbf{r}|^2/\hbar t \gg 1$.

Rewriting the semi-classical propagator (40) using (38) we have

$$K_t^{(sc)}(\mathbf{r}, \mathbf{r}_0|\mathbf{r}_1) = \sigma_{t,\tau_{sc}}(x, x_0) \frac{e^{\frac{imx^2}{2\hbar t}}}{(2i\pi\hbar t/m)^{1/2}} \frac{e^{\frac{im[(y-y_1)^2+(z-z_1)^2]}{2\hbar(t-\tau_{sc})}}}{2i\pi\hbar(t-\tau_{sc})/m} \frac{e^{\frac{im[y_1^2+z_1^2]}{2\hbar\tau_{sc}}}}{2i\pi\hbar\tau_{sc}/m}, \tag{41}$$

where the function $\sigma_{t,\tau_{sc}}$ is defined by

$$\sigma_{t,\tau_{sc}}(x, x_0) \equiv \frac{\lambda_0^2}{\rho} \left(\frac{-mx_0}{2\pi\hbar\tau_{sc}}\eta_1 + \frac{mx}{2\pi\hbar(t-\tau_{sc})}\eta_2\right) \tag{42}$$

and where $\rho \equiv |\mathbf{r}-\mathbf{r}_1| + |\mathbf{r}_1-\mathbf{r}_0|$ can be interpreted as the semi-classical path length traveled by the particle: see Fig. 1. Hence the one-slit propagator formula (28) can be written as follows:

$$K_{sc}^{(a,b)}(\mathbf{r}, t; \mathbf{r}_0, 0) = \frac{e^{\frac{imx^2}{2\hbar t}}}{(2i\pi\hbar t/m)^{1/2}} \int_{-a}^{a} dz_1 \int_{-b}^{b} dy_1\, \sigma_{t,\tau_{sc}}(x, x_0) \frac{e^{\frac{im[(y-y_1)^2+(z-z_1)^2]}{2\hbar(t-\tau_{sc})}}}{2i\pi\hbar(t-\tau_{sc})/m} \frac{e^{\frac{im[y_1^2+z_1^2]}{2\hbar\tau_{sc}}}}{2i\pi\hbar\tau_{sc}/m} \tag{43}$$

The formula (43) is similar to the one-point source propagator in the truncation approximation, formula (85) of Appendix 1, except that the semi-classical time τ_{sc} depends on the distance from the origin to the point in the slit, and from the slit to the screen (see (37)), and the function $\sigma_{t,\tau_{sc}}$ in front of the product of the two Gaussians depends on the boundary conditions.

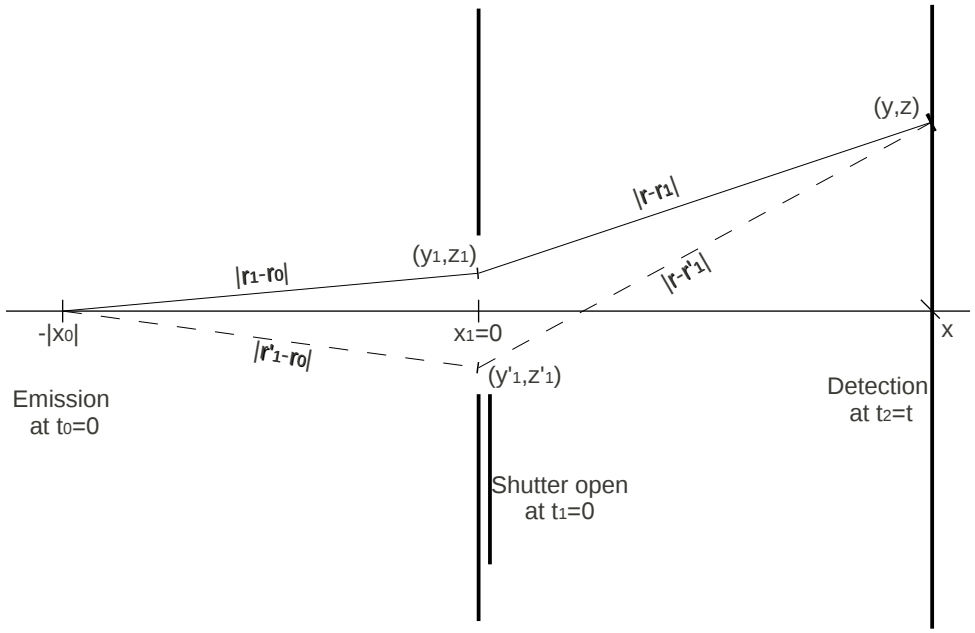

Figure 1: Schematic representation of the apparatus. We illustrate two interfering classical paths starting from $\mathbf{r}_0$ at the time $t_0 = 0$ to $\mathbf{r}$ at the time t and passing through the aperture at $\mathbf{r}_1$ (resp. $\mathbf{r}'_1$) at the time τ_{sc} (resp. τ'_{sc}) given by the formula (37).

Remark 1. We can give a geometric interpretation to the diffraction in space and in time in the semi-classical regime. The first-order term of the semi-classical approximation (41) gives only the classical path contribution. Therefore, we observe that the propagator (43) is nothing but a sum over all *semi-classical paths* (made up of two broken lines) passing through the aperture of the slit as in Fig.1. Thus, the equation (43) shows that the semi-

classical approximation is in fact a truncation approximation since one sees in these formulas that the motion along the x-axis and the motion in the orthogonal (y, z) plane are separated and moreover that along the x-axis the motion is classical. However, we have more information within our model since by (37) we notice that there is a relation between the classical times τ_{sc} and t even if the two motions from the source to the slit and from the slit to the screen are separated, see Fig. 1. Actually, we can interpret this relation as the conservation of the classical energy of the particle when the particle passes through the slit:

$$E(\mathbf{r}_1, \tau_{sc}) = E(\mathbf{r}, t) \Leftrightarrow \frac{m}{2}\left|\frac{\mathbf{r}_1 - \mathbf{r}_0}{\tau_{sc} - t_0}\right|^2 = \frac{m}{2}\left|\frac{\mathbf{r} - \mathbf{r}_1}{t - \tau_{sc}}\right|^2$$

and this leads to (37), whereas the classical momentum is not conserved due to the quantum diffraction phenomenon.

Consequently, in the semi-classical regime, the theory of diffraction in time allows us to take into account all the classical paths (passing through the slit at a time depending on the position inside the aperture) without assuming that the dimensions of the aperture are small compared to the dimension of the apparatus along the x-axis. Moreover, the additional term (42) which could not be discovered otherwise, has an important physical meaning since the values of the parameters $\eta_1,\ \eta_2$ depend on whether the screen of the slit is reflective, absorbing or neither.

In Fig.2., Appendix 3 we show the transition between the quantum and the semi-classical regimes from the left to the right.

Firstly, for the diffraction patterns at the left side (Fig.2.1a-2.4a), the *semi-classical parameter* $\mu \sim 4$ (i.e., relatively close to one) and so that explain why the curves are different from those for the truncation approximation (see Fig.2.4a). We observe that for the Dirichlet boundary condition (Fig.2.1a) there is a narrow central peak decreasing very fast so that we can not see the oscillations (a numerical zoom could show these slight oscillations). On the contrary, for the Neumann (Fig.2.2a) and the free boundary conditions (Fig.2.3a), there is no central peak but large oscillations where the distance between the fringes is essentially constant but different from the distance between the fringes in the truncation approximation (Fig.2.4a).

For the curves at right side of (Fig.2.1c-2.4c), we have $\mu \sim 800 \gg 1$ and then we get similar pictures to those in the truncation approximation (Fig. 2.4c) although there is still a difference in the location of the fringes. In the following section, we will give a qualitative description of those differences. From (72) and (76) we can conclude that if the first minima of the curves are not too different, however we observed that the second and the third differ by 50%.

The patterns in the middle of Fig.2, show the transition between the quantum and the semi-classical regimes where a central peak appears also for the Neumann (Fig.2.5) and the free boundary conditions (Fig.2.8).

Remark 2. Let us make another remark about the probabilistic interpretation of the slit diffraction experiment in the semi-classical limit. A consequence of the last comment about the relation between the semi-classical approximation and the truncation approximation is that there is an analogous equation to (26) giving the relation of the conservation of the probability between the aperture of the slit and the screen:

$$\int_{-b}^{b} dy_1 \int_{-a}^{a} dz_1 \ |\psi_{\rm sc}(\mathbf{r}_1, \tau_{sc})|^2 = \int_{-\infty}^{+\infty} dy \int_{-\infty}^{+\infty} dz \ |\psi_{\rm sc}(\mathbf{r}, t)|^2 \equiv M_{sc} \qquad (44)$$

where τ_{sc} is given by (37) and depends on $\mathbf{r}, \mathbf{r}_1, \mathbf{r}_0, t$, and where the semi-classical wave functions in (44) are given by:

$$\psi_{\rm sc}(\mathbf{r}_1, \tau_{sc}) = \int_{\mathbb{R}^3} d\mathbf{R} \ G_0(\mathbf{r}_1 - \mathbf{R}, \tau_{sc}) \frac{e^{i\frac{|\mathbf{R}-\mathbf{r}_0|^2}{2\sigma^2}}}{(2\pi\sigma^2)^{3/2}} \qquad (45)$$

$$\psi_{\rm sc}(\mathbf{r}, t) = \int_{\mathbb{R}^3} d\mathbf{R} \ K_{sc}^{(a,b)}(\mathbf{r}, t, \mathbf{R}, 0) \frac{e^{i\frac{|\mathbf{R}-\mathbf{r}_0|^2}{2\sigma^2}}}{(2\pi\sigma^2)^{3/2}} \qquad (46)$$

So we get the following formula for the semi-classical density of probability:

$$P_{sc}(\mathbf{r}, t) = \frac{1}{M_{sc}} |\psi_{sc}(\mathbf{r}, t)|^2 \to \frac{1}{\Omega_{sc}} |K_{sc}^{(a,b)}(\mathbf{r}, t, \mathbf{r}_0, 0)|^2, \text{ when } \sigma \to 0 \qquad (47)$$

where M_{sc} is defined in (44) and $\Omega_{sc} = \int_{-b}^{b} dy_1 \int_{-a}^{a} dz_1 \ |G_0(\mathbf{r}_1 - \mathbf{R}, \tau_{sc})|^2$.

4 Semi-classical approximations for the slit experiment

The equation (28) gives the three-dimensional one-gate-slit propagator as a double integral of the three-dimensional one-point-slit propagator given by the equations (30), (32) and (31). Despite the fact that there is no explicit formula giving the result for the gate-slit propagator, we can give an approximation when the size of the slit and the distance on the screen are relatively small, in which case it is also of interest to give an estimate for the relative shift between the minima in the interference pattern for the Fraunhofer regime compared with the truncation approximation.

We first want to give the semi-classical approximation of the one-point source propagator (30) when the sizes in the x-direction are relatively large compared to the sizes of the slit and of the distances of the observation point on the screen:

$$|x - x_1|, |x_1 - x_0| \gg a, b, |z|, |y|$$

and also large compared to $\lambda_0 = \sqrt{2\pi\hbar t/m}$ (relatively short time). Therefore the semi-classical limit (43) is a good approximation.

By (31), the phase of the propagator (30) is given by

$$\frac{\hbar}{m}\varphi_t = \frac{|\mathbf{r} - \mathbf{r}_1|^2}{2t} + \frac{|\mathbf{r}_1 - \mathbf{r}_0|^2}{2t} + \frac{|\mathbf{r} - \mathbf{r}_1||\mathbf{r}_1 - \mathbf{r}_0|}{t} \tag{48}$$

We denote the two-dimensional vectors of the position on the screen $\mathbf{r}_\perp = (y, z)$, on the slit $\mathbf{r}_{\perp,1} = (y_1, z_1)$. In the sequel, we take $x_1 = 0$, so $|x - x_1| = |x|$, $|x_1 - x_0| = |x_0|$ and $y_0 = 0,\ z_0 = 0,\ x_0 < 0$. The first two terms of the r.h.s. of (48) are rewritten as

$$\frac{|\mathbf{r} - \mathbf{r}_1|^2}{2t} + \frac{|\mathbf{r}_1|^2}{2t} = \frac{x^2}{2t} + \frac{(\mathbf{r}_\perp - \mathbf{r}_{\perp,1})^2}{2t} + \frac{x_0^2}{2t} + \frac{\mathbf{r}_{\perp,1}^2}{2t} \tag{49}$$

Expanding to fourth order the third term of the r.h.s. of (48), we have

$$\frac{|\mathbf{r} - \mathbf{r}_1||\mathbf{r}_1 - \mathbf{r}_0|}{t} = \frac{|x||x_0|}{t}\left(1 + \frac{(\mathbf{r}_\perp - \mathbf{r}_{\perp,1})^2}{x^2}\right)^{1/2}\left(1 + \frac{\mathbf{r}_{\perp,1}^2}{x_0^2}\right)^{1/2} \tag{50}$$

$$\approx \frac{|x||x_0|}{t}\left(1 + \frac{(\mathbf{r}_\perp - \mathbf{r}_{\perp,1})^2}{2x^2} - \frac{(\mathbf{r}_\perp - \mathbf{r}_{\perp,1})^4}{8x^4}\right)\left(1 + \frac{\mathbf{r}_{\perp,1}^2}{2x_0^2} - \frac{\mathbf{r}_{\perp,1}^4}{8x_0^4}\right) \tag{51}$$

$$\approx \frac{|x||x_0|}{t}\left(1 + \frac{\mathbf{r}_{\perp,1}^2}{2x_0^2} + \frac{(\mathbf{r}_\perp - \mathbf{r}_{\perp,1})^2}{2x^2}\right) - \frac{|x||x_0|}{8t}\left(\frac{(\mathbf{r}_\perp - \mathbf{r}_{\perp,1})^2}{x^2} - \frac{\mathbf{r}_{\perp,1}^2}{x_0^2}\right)^2 \tag{52}$$

Due to (49) and (52) we get:

$$\frac{\hbar}{m}\varphi_t \approx \frac{(x - x_0)^2}{2t} + \frac{(\mathbf{r}_\perp - \mathbf{r}_{\perp,1})^2}{2(t - t_c)} + \frac{\mathbf{r}_{\perp,1}^2}{2t_c} - \frac{|x||x_0|}{8t}\left(\frac{(\mathbf{r}_\perp - \mathbf{r}_{\perp,1})^2}{x^2} - \frac{\mathbf{r}_{\perp,1}^2}{x_0^4}\right)^2 \tag{53}$$

where:

$$t_c = \frac{|x_0|}{|x| + |x_0|}t = \frac{|x_0|}{|x - x_0|}t\ . \tag{54}$$

4.1 The truncation approximation

Notice that due to (37), t_c could be interpreted as the semi-classical time at the first order approximation in the regime $|x|, |x_0| \gg |z|, |z_1|$:

$$\tau_{sc} = \frac{|\mathbf{r}_1 - \mathbf{r}_0| t}{|\mathbf{r} - \mathbf{r}_1| + |\mathbf{r}_1 - \mathbf{r}_0|} \approx t_c, \text{ when } |x|, |x_0| \gg |z|, |z_1| \ . \tag{55}$$

Inserting this into the amplitude of (41), i.e. neglecting the influence of the position on the screen and in the slit, we get the following approximation:

$$A_t(\mathbf{r}, \mathbf{r}_0|\mathbf{r}_1) \approx \sigma_{t,t_c}(x, x_0) \frac{1}{\sqrt{2i\pi\hbar t/m}} \frac{1}{(2i\pi\hbar/m)^2 (t - t_c) t_c} \ . \tag{56}$$

where $\sigma_{t,t_c}(x, x_0)$ is given by (42). In (53), we neglect the terms of order $O(\mathbf{r}_\perp^4)$ and $O(\mathbf{r}_{\perp,1}^4)$, to get

$$\frac{\hbar}{m} \varphi_t \approx \frac{(x - x_0)^2}{2t} + \frac{(\mathbf{r}_\perp - \mathbf{r}_{\perp,1})^2}{2(t - t_c)} + \frac{\mathbf{r}_{\perp,1}^2}{2t_c} \ . \tag{57}$$

Then, by (56) and (57), we get the Fraunhofer approximation to second order for the one-point source propagator:

$$K_t(\mathbf{r}, \mathbf{r}_0|\mathbf{r}_1) \approx$$
$$\sigma_{t,t_c}(x, x_0) \frac{e^{im\frac{(x-x_0)^2}{2\hbar t}}}{\sqrt{2i\pi\hbar t/m}} \frac{e^{im\frac{(y-y_1)^2}{2\hbar(t-t_c)}}}{\sqrt{2i\pi\hbar(t-t_c)/m}} \frac{e^{im\frac{y_1^2}{2\hbar t_c}}}{\sqrt{2i\pi\hbar t_c/m}} \frac{e^{im\frac{(z-z_1)^2}{2\hbar(t-t_c)}}}{\sqrt{2i\pi\hbar(t-t_c)/m}} \frac{e^{im\frac{z_1^2}{2\hbar t_c}}}{\sqrt{2i\pi\hbar t_c/m}} \ . \tag{58}$$

Consequently, for the single-slit model, by integrating over y_1, z_1 on $[-b, b] \times [-a, a]$, we get the usual truncation approximation formula (86), see Appendix 1, multiplied by a constant factor σ_{t,t_c} depending on t and t_c, as well as on $|x_0|$, x and on the boundary conditions. In addition, by the semi-classical probabilistic interpretation, see (47), since $\sigma_{t,t_c}(x, x_0)$ is a constant number, we get the same probability density formula as the one in [14], (see also (96) in Appendix 1) which means that the initial boundary conditions on the slit do not affect the diffraction pattern in this regime. We observe this phenomenon numerically in Fig.3. for $t = 0.05$ and $t = 0.005$.

4.2 The fourth-order approximation in the Fraunhofer regime

Remember that the Fresnel numbers (see Appendix 1) are given by

$$N_F(a) = \frac{2a^2}{\lambda L}, \ N_F(b) = \frac{2b^2}{\lambda L}$$

where $L = |x|$ and $\lambda = 2\pi\hbar/(mv)$, and where a is the dimension of the slit along the z-axis and b the one along the y-axis, with $v \approx v_x = |x - x_0|/t$. In the Fraunhofer regime, we have $N_F(a) \ll 1$ and since the distance between two successive minima on the pattern is $\Delta z \sim \lambda L/(2a) = a/N_f(a)$ (see Fig. 3 for the truncation model (TM) and [14]), we have $\Delta z \gg a$ and so we are looking for the correction for $z \gg a$. We also assume that $x \gg b \gg a$ and $2b^2/(\lambda L) \ll 1$, so that $\Delta z \gg \Delta y \gg b$. In this case, we can neglect the terms of the order $O(y^4)$ and $O(y_1^4)$ in (53):

$$\frac{\hbar}{m}\varphi_t \approx \frac{x^2}{2t} + \frac{(\mathbf{r}_\perp - \mathbf{r}_{\perp,1})^2}{2(t-t_c)} + \frac{\mathbf{r}_{\perp,1}^2}{2t_c} - \frac{|x||x_0|}{8t}\left(\frac{(z-z_1)^2}{x^2} - \frac{z_1^2}{x_0^2}\right)^2 \tag{59}$$

given that $z \gg a \geq z_1$, we get

$$\left(\frac{(z-z_1)^2}{x^2} - \frac{z_1^2}{x_0^2}\right)^2 \approx \frac{(z^2 - 2z_1 z)^2}{x^4} \tag{60}$$

which means that we keep only the terms of the order $O(z^2 z_1^2)$ (plus the terms of the order z^4) and we neglect the terms of the order $O(z_1^4)$. Inserting the approximation (60) in (59), we obtain:

$$\frac{\hbar}{m}\varphi_t \approx \frac{x^2}{2t} + \frac{(y-y_1)^2}{2(t-t_c)} + \frac{y_1^2}{2t_c} + \frac{(z-z_1)^2}{2(t-t_c)} + \frac{z_1^2}{2t_c} - \frac{|x_0|z^2}{8|x|^3 t}(2z_1 - z)^2 \ , \tag{61}$$

which leads to a similar expression to the second order expanding of the phase (57) after rewriting the last three terms of (61) in another explicit form:

$$\frac{\hbar}{m}\varphi_t \approx \frac{x^2}{2t} + \frac{(y-y_1)^2}{2(t-t_c)} + \frac{y_1^2}{2t_c} + \frac{(z-z_1^{'})^2}{2(t'-t_c')} + \frac{z_1'^2}{2t_c'} - \frac{z^4}{8|x|^2}\frac{t_c}{t(t-t_c)} \ , \tag{62}$$

where we used the expression (54), and where

$$t_c^{'} = t_c\left(1 - \frac{t_c}{2t}\frac{z^2}{x^2}\right)^2\left(1 + \frac{4t_c^3}{(t-t_c)^2 t}\frac{z^4}{x^4}\right)^{-1} \approx t_c\left(1 - \frac{z^2}{|x|^2}\frac{t_c}{t}\right) \ , \tag{63}$$

$$t' - t_c^{'} = t - t_c \ , \tag{64}$$

$$z_1^{'} = z_1\left(1 - \frac{z^2}{2|x|^2}\frac{t_c}{t}\right) \ . \tag{65}$$

Here we approximated (63) to the second order $O(\frac{z}{x})^2$ such that $\frac{z_1'^2}{2t_1'}$ is of the fourth order $O(\frac{z}{x})^4$. We remark that the term $\theta\frac{z^2}{2t}$, $\theta \equiv -\frac{z^2}{4|x|^2}\frac{t_c}{(t-t_c)}$

appearing in (62) gives no contribution to the intensity. Keeping the zeroth-order approximation for the amplitude (56), the fourth -order approximation gives the propagator in the z-direction :

$$e^{im\theta\frac{z^2}{2\hbar t}}\int_{-a}^{a}dz_1\frac{e^{im\frac{x^2}{2\hbar t}}}{\sqrt{2i\pi\hbar t/m}}\frac{e^{im\frac{(z-z_1^{'})^2}{2\hbar(t^{'}-t_c^{'})}}}{\sqrt{2i\pi\hbar(t-t_c)/m}}\frac{e^{im\frac{z_1^{'2}}{2\hbar t_c}}}{\sqrt{2i\pi\hbar t_c/m}}$$

$$=e^{im\theta\frac{z^2}{2\hbar t}}\int_{-a'}^{a'}dz_1^{'}\frac{e^{im\frac{x^2}{2\hbar t}}}{\sqrt{2i\pi\hbar t/m}}\frac{e^{im\frac{(z-z_1^{'})^2}{2\hbar(t^{'}-t_c^{'})}}}{\sqrt{2i\pi\hbar(t^{'}-t_c^{'})/m}}\frac{e^{im\frac{z_1^{'2}}{2\hbar t_c^{'}}}}{\sqrt{2i\pi\hbar t_c^{'}/m}} \quad (66)$$

since $dz_1^{'}/\sqrt{t_c^{'}}\approx dz_1/\sqrt{t_c}$ by (63) and since $\sqrt{1+\epsilon^2}\approx 1+\frac{\epsilon^2}{2}$, for $\epsilon\ll 1$. Thus we obtain a similar result to (86):

$$\widetilde{K}_{t,t_c}(x,y,z;b,a)=\sigma_{t,t_c}(x,x_0)\frac{e^{im\frac{(x^2+y^2+z^2)}{2\hbar t}}}{(2i\pi\hbar t/m)^{3/2}}F_{t^{'},t_c^{'}}(z,a^{'})F_{t,t_c}(y,b), \quad (67)$$

where the function $F_{t^{'},t_c^{'}}$ is defined by (87), and where $\alpha_{t^{'},t_c^{'}}$ is given by

$$\alpha_{t^{'},t_c^{'}}(z,a^{'})=\left(\frac{2a^{'2}}{2\pi\hbar t_c(t-t_c)/mt}\right)^{1/2}\left(1-\frac{z}{a^{'}}\frac{t_c}{t}\right)=\alpha_{t,t_c}(z,a^{'})\ . \quad (68)$$

Similar to (91), since $\lambda\approx 2\pi\hbar/mv_x$ with $v_x=|x-x_0|/t$ and $t_c\approx|x_0|/v_x=|x_0|t/|x-x_0|$, we can rewrite (68) as

$$\alpha_{t^{'},t_c^{'}}(z,a^{'})\equiv\sqrt{\gamma N_F^{'}}\left(1-\frac{z}{a^{'}\gamma}\right),\ \gamma=|x-x_0|/|x_0| \quad (69)$$

where the Fresnel number is:

$$N_F^{'}\equiv\frac{2a^{'2}}{\lambda L}\approx N_F\times\left(1-\frac{z^2}{\gamma L^2}\right)\ , \quad (70)$$

where $L=|x|$ and $\gamma=|x-x_0|/|x_0|$ (and we have used $t_c/t\approx|x_0|/|x-x_0|$). By (67), we find an analogous result for the distance Δz between two successive minima of the intensity (see [14] for a detailed approximation) but to fourth-order approximation:

$$\Delta z^{'}\approx\frac{\lambda L}{2a^{'}}\approx\Delta z\left(1+\frac{z^2}{2\gamma L^2}\right)\ . \quad (71)$$

Thus, we should observe in the intensity pattern (see Fig.2c), a deviation of the distance between the consecutive minima from the truncation approximation given by the following law:

$$\delta\equiv\frac{\Delta z^{'}-\Delta z}{\Delta z}\approx\frac{z^2}{2\gamma L^2}. \quad (72)$$

4.3 Criterion for the validity of the fourth-order approximation

As we saw in the last Section IV.B, the 4th-order correction involves the ratio between the distance of the observation on the screen and the distance in the x-direction between the screen and the slit. The aim of this section is to understand the condition of validity for the 4th -order correction to the truncation approximation model. Here we have to assume that the system is in the semi-classical regime so that the parameter μ, introduced in Section III.B is relatively small. Hence we will see that the corrections are not related to the value of the parameter μ but to the quantum fluctuation along the x-axis.

We remark that in Fig.3, Appendix 3 the approximation seems valid for the curves at the right side (Fig.3.1c-3.3c compared with Fig.3.4c) and at the middle (Fig.3.1b-3.3b compared with Fig.3.4b), whereas it is not correct for the curves at the left side (Fig.3.1a-3.3a compared with Fig.3.4a). Actually, the optical resolution of the pattern has to be high enough to distinguish two successive minima, i.e. the relative difference δ, see (72), has to be small :

$$\delta \lll 1 \Rightarrow z \ll L\sqrt{2\gamma} \tag{73}$$

This means that the distance z on the screen has to be relatively small compared to L (if $\gamma \sim 1/2$). We have seen that in the Fraunhofer regime (see Appendix 1 and [14] for more details) the pattern on the screen has several minima at $n\Delta z$, $n = 2, 3, 4, \cdots$ with distances $\Delta z = \lambda L/2a$. In fact, for $z \gg \Delta z$, the intensity becomes rather small compared to its maximum and so the visibility is low. If we consider that we can observe the pattern in a window $|z| \leq n\Delta z$, then by (73) we get the criterion

$$\Delta z \ll L\frac{\sqrt{2\gamma}}{n} \Rightarrow \frac{\lambda}{L} \ll \frac{a}{L}\frac{\sqrt{8\gamma}}{n} \tag{74}$$

Hence, given the geometrical parameter a/L, we obtain a condition for the ratio between the wavelength $\lambda = 2\pi\hbar/mv \approx 2\pi\hbar t/(m|x - x_0|)$ and the distance L. We reintroduce the parameter $\lambda_0 = \left(\frac{2\pi\hbar t}{m}\right)^{1/2}$, so that $\lambda = \frac{\lambda_0^2}{|x-x_0|}$. The length λ_0 can be interpreted as the spatial fluctuation of the phase $\exp(im|x-x_0|^2/2\hbar t) = \exp\left(i\pi|x - x_0|^2/\lambda_0^2\right)$ appearing in the free propagator (4). So if t is small enough, then $\lambda/|x - x_0| = \lambda_0^2/|x - x_0|^2$ will be very small and consequently the space fluctuations in the x-axis will be negligible. On the contrary, if t is large, the fluctuations are not negligible and then the approximation $\lambda \ll |x-x_0|$ is not valid. The criterion (74) gives a condition:

$$\frac{\lambda_0^2}{|x - x_0|^2} \ll \frac{1}{n}\frac{a}{L}\left(\frac{8\gamma}{\gamma'}\right)^{1/2} \Leftrightarrow q \ll \frac{1}{n} \tag{75}$$

where the parameter called the *coherence number in the x-direction* q is defined as

$$q \equiv \frac{\kappa^2}{\rho} \tag{76}$$

where $\kappa \equiv \lambda_0/|x-x_0|$ is the *quantum fluctuation parameter in the x-axis* and $\rho \equiv \frac{a}{L}\left(\frac{8\gamma}{\gamma'}\right)^{1/2}$ with $\gamma' = |x-x_0|/L$, is the inverse of the *zoom parameter*.

In the Fig.3, Appendix 3 for the diffraction patterns at the left side (Fig.3.1a-3.4a) the coherence parameter is of the order of unity, and the semi-classical parameter $\mu \sim 2500$ (with $N_F(a) \sim 3 \times 10^{-5}$, $N_F(b) \sim 3 \times 10^{-3}$). We observe some differences with the truncation approximation. First, the distance between the fringes is about 66% in case of the first minimum and 100% for the second. We conclude that in those cases, the fourth-order approximation above is not valid. However, we observe different shapes for the different boundary conditions and also the amplitude of the oscillations are not the same. If we suppose that we can experimentally (and this is probably a big challenge) build an apparatus for which the parameter μ is of the range $10^2 - 10^4$, the differences described before would provide physical information about the surface of the slit.

For the Fig.3.1b-3.4b, the parameters $q \sim 6 \times 10^{-2}$ and $\mu \sim 5 \times 10^4$ (with $N_F(a) \sim 6 \times 10^{-4}$, $N_F(b) \sim 3 \times 10^{-2}$). In this case the fourth-order approximation is quite good for the first ten fringes. For example, we have $\delta \sim 0.1\%$ for the first fringe' shift, $\delta \sim 7\%$ for the third one and $\delta \sim 16\%$ for the fifth one. Additionally, we observe that the shape of the curves as well as the amplitude of the oscillations do not depend on the boundary conditions.

Similarly for the Fig.3.1c-3.4c, the parameters $q \sim 6\times10^{-3}$ and $\mu \sim 5\times10^5$ (with $N_F(a) \sim 6\times10^{-3}$, $N_F(b) \sim 6\times10^{-1}$) and we obtain diffraction patterns very close to the truncation approximation. In the next section, we will see that experimentally this is the general situation.

5 Discussion

5.1 General remarks

Concerning the two-slit problem, we observed that for large μ and for small Fresnel numbers ($N_F(a), N_F(b), N_F(d) \ll 1$, where d is the distance between the centers of the slits along the z-axis) the interference pattern has a similar shape to the one for the truncation approximation (see [14]), see Fig. 4, Appendix 3 but we observe a similar diffraction in time phenomenon for the envelope of the interference pattern which is nothing but the diffraction

curve for a single-slit centered at $x_1 = y_1 = z_1 = 0$. The two-slit propagator formula is given by:

$$K^{(dble)}(\mathbf{r},t,\mathbf{r}_0,0) = \int_{-a-d}^{-a+d} dz_1 \int_{-b}^{b} dy_1\, K(\mathbf{r},t;\mathbf{r}_0,0|\mathbf{r}_1) + \int_{a-d}^{a+d} dz_1 \int_{-b}^{b} dy_1\, K(\mathbf{r},t;\mathbf{r}_0,0|\mathbf{r}_1) \tag{77}$$

where the three-dimensional one-point source propagator $K(\mathbf{r},t;\mathbf{r}_0,0|\mathbf{r}_1)$ is given by (30).

Here we have only studied a rectangular aperture but naturally the propagator (24) can be generalized for an arbitrarily shape of slit:

$$K^{(\Sigma)}(\mathbf{r},t,\mathbf{r}_0,0) = \int_{\Sigma} dy_1 dz_1\; K(\mathbf{r},t;\mathbf{r}_0,0|\mathbf{r}_1) \tag{78}$$

where Σ is the aperture of the slit (e.g., circle) and where the one-point source propagator $K(\mathbf{r},t;\mathbf{r}_0,0|\mathbf{r}_1)$ is given by (30).

Also, we mention that the semi-classical approximation is valid for two dimensions where we have to integrate (24) along the y_1-axis and apply the stationary phase approximation method. Similarly to (43) we get:

$$K_{sc}^{(2D)}(\mathbf{r},t;\mathbf{r}_0,0) = \frac{e^{\frac{imx^2}{2\hbar t}}}{\sqrt{2i\pi\hbar t/m}} \int_{-a}^{a} dz_1\, \sigma_{t,\tau_{sc}}^{(2D)}(x,x_0) \frac{e^{\frac{im(z-z_1)^2}{2\hbar(t-\tau_{sc})}}}{\sqrt{2i\pi\hbar(t-\tau_{sc})/m}} \frac{e^{\frac{im(z_1-z_0)^2}{2\hbar\tau_{sc}}}}{\sqrt{2i\pi\hbar\tau_{sc}/m}} \tag{79}$$

where $\sigma_{t,\tau_{sc}}^{(2D)}(x,x_0)$ is given by (42) and with the semi-classical time τ_{sc} is given by (37) taking $y_0 = y_1 = y = 0$.

5.2 Ultracold atoms slit experiment under gravity

In the slit experiments for electrons, cold neutrons and heavy molecules, we point out that the dimensions of the apparatus are large so that the semi-classical parameter is very large, for example in [9] and [7], μ is of the order $\sim 10^{10}$, it is $\sim 10^{13}$ in [11] and $\sim 10^{7}$ in [10]. Additionally, experimentally the initial wave function (at the time of the emission) is not localized at $\mathbf{r}_0$ but a plane wave along the x-axis. As discussed above, it suffices to Fourier transform the propagator (28) with respect to the variable x_0. However, in the cold atoms experiment [10] the narrow wave packet model is more convenient even if for realistic conditions we do not reach the limit $\sigma \to 0$. In [28] is presented a theoretical description and interpretation of the latter experiment, but still following the truncation approximation. Concretely, a bunch of coherent cold neon atoms (mass $m = 3.349 \times 10^{-26}$kg) is trapped

above a plate where there are two apertures (the two-slits system) at a distance l_1. At the time $t_0 = 0$ the optical-magnetic trap is switch off and the atoms fall under the gravity field of the earth, passing through the two slits and strike a detection plate at distance l_2 from the two-slit plate. It is assumed that the initial wave of an atom falling down the gravity field is a Gaussian wave packet centered at $\mathbf{r}_0 = \mathbf{0}$ with an initial vector wave $\mathbf{k}_0$. It is also assumed that the motion along the z-axis is classical. Moreover, the dimensions of the slits are considered to be small compared to the distances l_1 and l_2 which, in addition to the classical treatment along z, is the truncation approximation. By fixing $k_{0,z} = 0$, it follows that the classical time that the particle needs to pass through the slits is simply given by $t_1 = \sqrt{2l_1/g}$. Then, taking $l_1 \sim 0.1$m, $g = 9.81\text{ms}^{-2}$ we compute $t_1 \sim 0.1$s and so $\lambda \approx \hbar/mv_z \sim 1.5 \times 10^{-8}$m which yields to $\mu \approx 2\pi(l_1 + l_2)/\lambda \sim 10^7$. Besides, in [28] numerical simulations are performed to study the probability density for small l_2 showing that the interference patterns can be observed only for $l_2 \geq 5 \times 10^{-4}$m. In the Fig. 4 of [28], the probability density is plotted especially for $l_1 = 10^{-4}$m, 5×10^{-4}m, 10^{-3}m, 1.13×10^{-1}m where we can observe a transition between the so-called *separated regime* and the *mixed regime* [14] between the two-slits patterns. However the length l_1 was kept fixed for numerical simulation and so we may wonder what the shape pattern would be if we varied the length l_1 in such a way that the total length $l_1 + l_2$ is of orders $10^{-6} - 10^{-2}$m. In this situation, the semi-classical parameter μ would be of orders $10^2 - 10^6$ and so we expect the probability density to be modified by the fluctuation along the z-axis which should exhibit a correction to the truncation approximation model.

Here we will give a brief description of the modifications needed in our model to describe this experiment. Again we use the Brunker-Zeilinger method and obtain a semi-classical approximation for the propagator. We leave the numerical simulation for another article where we will investigate the phenomenological consequences of our model.

As described above, we consider Gaussian wave packet (10) centered at $x_0 = y_0 = z_0 = 0$ falling down the gravity field $\mathbf{g} = g\,\mathbf{e}_z$ where $g = 9.81\text{ ms}^{-1}$ and passing through a single slit, where the slit is an aperture in a plane orthogonal to the z-axis positioned at $z_1 > 0$. After a time t, the particle is detected on a screen at the position $z > z_1$. We describe the quantum-motion of the particle by the following equation similar to (1):

$$\begin{array}{l} -\frac{\hbar^2}{2m}\nabla^2\psi(\mathbf{r},t) + V(z)\ \psi(\mathbf{r},t) = i\hbar\frac{\partial}{\partial t}\psi(\mathbf{r},t) \\ \psi(\mathbf{r},t) = 0 \text{ for } z > z_1 \text{ and } t < t_1, \text{ and } \psi(\mathbf{r}_1,t) = \phi(\mathbf{r}_1,t) \text{ for } t > t_1. \end{array} \tag{80}$$

with $V(z) = mgz$ and where we fixed the boundary and initial condition on

the plane of the slit. As before, we consider a shutter opening at the time $t_1 = 0$ after which the wave propagates below the slit plane (i.e. $z > z_1$).

Using the same arguments as previously but replacing the free Green's function by:

$$G_g(\mathbf{r}, t; \mathbf{r}', t') = G_0(\mathbf{r}, t; \mathbf{r}', t')\ e^{\frac{im}{2\hbar}\left(g(z+z')(t-t') - \frac{g^2}{12}(t-t')^3\right)} \tag{81}$$

where the free propagator $G_0(\mathbf{r}, t; \mathbf{r}', t')$ is given by (4), we get:

$$K^{(g)}(\mathbf{r}, t; \mathbf{0}, 0) = \frac{i\hbar}{2m} \int_0^t d\tau \int_{-a}^{a} dz_1 \int_{-b}^{b} dy_1\ \chi_{t,\tau}(z, z_1) G_g(\mathbf{r}, t; \mathbf{r}_1, \tau) G_g(\mathbf{r}_1, t; \mathbf{0}, \tau) \tag{82}$$

where:

$$\chi_{t,\tau}(z, z_1) \equiv \eta_1 \frac{z_1}{\tau} + \eta_2 \frac{z - z_1}{t - \tau} - i\eta_2\ gt + i(\eta_1 + \eta_2) g\tau - i(\eta_1 - \eta_2) \frac{g\tau}{2}$$

Then for $\mu \equiv m\mathbf{r}^2/(2\hbar t) \gg 1$, by the stationary phase approximation we obtain:

$$K_{sc}^{(g)}(\mathbf{r}, t; \mathbf{0}, 0) \approx \int_{-a}^{a} dx_1 \int_{-b}^{b} dy_1\ A_{sc}(\mathbf{r}, t; \mathbf{0}, 0|\mathbf{r}_1)\ e^{i\phi_{sc}(\mathbf{r}, t; \mathbf{0}, 0)|\mathbf{r}_1)} \tag{83}$$

where the one-point source amplitude is given by

$$A_{sc}(\mathbf{r}, t; \mathbf{0}, 0|\mathbf{r}_1) = \frac{\chi_{t,\tau_{sc}}(z, z_1)}{((2i\pi\hbar/m)^2 (t - \tau_{sc})\tau_{sc})^{3/2}} \left(\frac{2i\pi}{\omega_{sc}(\mathbf{r}, t; \mathbf{0}, 0)}\right)^{1/2}$$

with

$$\omega_{sc}(\mathbf{r}, t; \mathbf{0}, 0|\mathbf{r}_1) = \frac{m}{\hbar} \left(\frac{(\mathbf{r} - \mathbf{r}_1)^2}{(t - \tau_{sc})^3} + \frac{|\mathbf{r}_1|^2}{(\tau_{sc} - t_0)^3}\right) - \frac{mg^2 t}{4\hbar}$$

and the one-point source phase by

$$\phi_{sc}(\mathbf{r}, t; \mathbf{0}, 0|\mathbf{r}_1) = \frac{m}{2\hbar} \left(\frac{(\mathbf{r} - \mathbf{r}_1)^2}{t - \tau_{sc}} + \frac{|\mathbf{r}_1|^2}{\tau_{sc} - t_0}\right)$$
$$+ \frac{m}{2\hbar} \left(g(z + z_1)(t - \tau_{sc}) + (z_1)(\tau_{sc} - t_0) - \frac{g^2}{12}(t - \tau_{sc})^3 - \frac{g^2}{12}(\tau_{sc} - t_0)^3\right)$$

Here, the semi-classical time τ_{sc} is the solution of the following fifth-order polynomial equation (since after expansion, the term in τ^6 disappears):

$$(\mathbf{r} - \mathbf{r}_1)^2 \tau^2 - |\mathbf{r}_1|^2 (t - \tau)^2 = gz(t - \tau)^2 \tau^2 + \frac{g^2}{4} \tau^4 (t - \tau)^2 - \frac{g^2}{4} \tau^2 (t - \tau)^4 \tag{84}$$

which can be interpreted as the conservation of the classical energy of the particle passing through the aperture, the trajectories being two broken parabolas similarly to the broken straight lines for the case without gravity. The first parabolic trajectory goes from $\mathbf{r}_0 = \mathbf{0}$ at the time $t_0 = 0$ to the point $\mathbf{r}_1$ at the time τ, and the second one from $\mathbf{r}_1$ at the time τ to the point $\mathbf{r}$ at the time t. Then, the classical energies for a particle following the two trajectories are $E_0 = \frac{m}{2}\mathbf{v}_0^2$ for the first one and $E_1 = \frac{m}{2}\mathbf{v}_1^2 - mgz_1$ for the second one, with the classical velocities

$$\mathbf{v}_0 = \frac{x_1 - x_0}{\tau - t_0}\mathbf{e}_x + \frac{y_1 - y_0}{\tau - t_0}\mathbf{e}_y + (\frac{z_1}{\tau - t_0} - \frac{g}{2}(\tau - t_0))\mathbf{e}_z$$

$$\mathbf{v}_0 = \frac{x - x_1}{t - \tau}\mathbf{e}_x + \frac{y - y_1}{t - \tau}\mathbf{e}_y + (\frac{z - z_1}{t - \tau} - \frac{g}{2}(t - \tau))\mathbf{e}_z$$

The conservation of energy equation

$$E_0 = E_1 \Leftrightarrow \frac{1}{2}|\mathbf{v}_0|^2 = \frac{1}{2}|\mathbf{v}_1|^2 - gz_1$$

then leads to the equation (84).

5.3 Conclusion

To summarize, the fourth-order corrections are generally small for realistic experimental situations, which is to be expected a priori since the theoretical predictions fit very well with the past and current experiments. However, our model brings a new perspective investigating the quantum diffraction beyond the truncation approximation. The fluctuation along the "propagation axis" could in principle be quantitatively and qualitatively demonstrated experimentally for a system following the conditions (minimum):

1. the apparatus has to be of mesoscopic scale, since we have seen that the length along the "propagation axis" has to be of orders $10^{-6} - 10^{-3}$m to have $\mu \sim 10^2 - 10^5$ in order to be able to observe any shift in the distances between the fringes.

2. the statistics have to be high enough to have a good accuracy so that we can detect a shift for $\delta \sim 10\%$ and also so that the differences between the amplitude of the oscillation for different boundary conditions can be detected.

To construct an experimental apparatus of this kind is certainly a challenge but perhaps not entirely beyond future advances in technology.

6 Appendices

6.1 Appendix 1: The truncation approximation for the quantum-multi-slit diffraction problem

We recall[14] that the single "gate" slit propagator, centered on the x-axis of size $2a$ on the z-axis and $2b$ on the y-axis is given by the following formula [14]:

$$K^{(a,b)}_{\text{Trunc}}(\mathbf{r},t;\mathbf{r}_0,0|\mathbf{r}_1,t_c)=\frac{e^{i\frac{m(x-x_0)^2}{2\hbar t}}}{(2i\pi\hbar t/m)^{1/2}}\int_{-a}^{a}dz_1\int_{-b}^{b}dy_1\frac{e^{i\frac{m[(y-y_1)^2+(z-z_1)^2]}{2\hbar(t-t_c)}}}{2i\pi\hbar(t-t_c)/m}\frac{e^{i\frac{m[(y_1-y_0)^2+(z_1-z_0)^2]}{2\hbar t_c}}}{2i\pi\hbar t_c/m}\ , \tag{85}$$

where $t_c=|x_1-x_0|t/|x-x_0|$. We note that this formula is valid only if the distances on the x-axis are very large compared to the distance on the screen and to the sizes of the slit, i.e. for $|x-x_1|,|x_1-x_0|\gg a,b,|y|,|z|$.[14] The formula (85) can be interpreted as follows: The propagator is the sum over the paths $x(\tau)$ of the particle going from the source $(x(0)=x_0,z(0)=z_0,y(0)=y_0)$ to the screen $(x(t)=x,z(t)=z,y(t)=y)$, given that it goes through the slit $x(t_c)=x_1,\ z(t_c)=z_1\in[-a,a],\ y(t_c)=y_1\in[-b,b]$ at the time t_c defined just above. Notice that we can find an explicit formula for the propagator (85) in terms of the Fresnel function [12], [14]:

$$K^{(a,b)}_{\text{Trunc}}(\mathbf{r},t;\mathbf{r}_0,0|\mathbf{r}_1,t_c)=\frac{e^{i\frac{|\mathbf{r}-\mathbf{r}_0|^2}{2t}}}{(2i\pi\hbar t/m)^{3/2}}F_{t,t_c}(z,a)F_{t,t_c}(y,b) \tag{86}$$

where:

$$F_{t,t_c}(z,a)\equiv(C[\alpha_{t,t_c}(z,a)]+C[\alpha_{t,t_c}(z,-a)]+iS[\alpha_{t,t_c}(z,a)]+iS[\alpha_{t,t_c}(z,-a)]) \tag{87}$$

and where the Fresnel functions are defined as follows [29]:

$$u\in\mathbb{R}^1\mapsto C[u]=\int_0^u dw\ \cos(\frac{\pi w^2}{2}) \tag{88}$$

$$u\in\mathbb{R}^1\mapsto S[u]=\int_0^u dw\ \sin(\frac{\pi w^2}{2}) \tag{89}$$

with

$$\alpha_{t,t_c}(z,a)\equiv\left(\frac{ma^2t}{\pi\hbar t_c(t-t_c)}\right)^{1/2}\left(1-\frac{z}{a}\frac{t_c}{t}\right) \tag{90}$$

and since we have seen that $\lambda\approx 2\pi\hbar/mv_x$ with $v_x=|x-x_0|/t$ and $t_c\approx|x_1-x_0|/v_x=|x_1-x_0|t/|x-x_0|$, we can rewrite (90) as

$$\alpha_{t,t_c}(z,a)\equiv\sqrt{\gamma N_F}\left(1-\frac{z}{a\gamma}\right)\ , \tag{91}$$

where $\gamma = |x - x_0|/|x_1 - x_0|$ and where the Fresnel number is defined as

$$N_F \equiv \frac{2a^2}{\lambda L} \ , \tag{92}$$

where $L = |x - x_1|$.

The intensity on the screen is proportional to the modulus square of the propagator, and is given by[14]:

$$I^{(a,b)}_{\rm Trunc}(\mathbf{r}, t; \mathbf{r}_0, 0|\mathbf{r}_1, t_c)| \equiv I_0 |K^{(a,b)}_{\rm Trunc}(\mathbf{r}, t; \mathbf{r}_0, 0|\mathbf{r}_1, t_c)|^2 = I_0 \left(\frac{m}{2\pi\hbar t}\right)^3 |F_{t,t_c}(z, a)|^2 |F_{t,t_c}(y, b)|^2 \tag{93}$$

In [14] three distinct regimes were considered depending on the value of the Fresnel number:
(i) If $N_F \ll 1$: we have the *Fraunhofer regime*, which means that the distances are sufficiently large to get a usual interference pattern [30] where the distance between two consecutive minima of intensity are about $\lambda L/(2a)$ in the z-direction and $\lambda L/(2b)$ in the y-direction.
(ii) If $N_F \gg 1$: we are in the so-called *Fresnel regime* where the interference pattern has a similar shape as the gate but with a different scale: $a(\gamma - 1)$ in the z-direction and $b(\gamma - 1)$ in the y-direction. More specifically, the intensity is very small if $z > a(\gamma - 1)$ and $y > b(\gamma - 1)$ and oscillate very fast around a constant if $z < a(\gamma - 1)$ and $y < b(\gamma - 1)$.
(iii) If $N_F \sim 1$: the *intermediate regime* is a transition between both regimes for which there is a spreading around the center of the intensity and similar to the Fraunhofer regime for large distances (on the screen).

The formula for the multi-slit problem is given by the sum over the single-slit propagator for each slit (centered in (A_j, B_j), $j = 1, .., N$):

$$K^{(N)}_{\rm Trunc}(\mathbf{r}, t; \mathbf{r}_0, 0|\mathbf{r}_1, t_c) = \frac{e^{i\frac{m(x-x_0)^2}{2\hbar t}}}{(2i\pi\hbar t/m)^{1/2}} \sum_{j=1}^{N} \int_{A_j-a_j}^{A_j+a_j} \int_{B_j-b_j}^{B_j+b_j} \frac{e^{i\frac{m[(y-y_1)^2+(z-z_1)^2]}{2\hbar(t-t_c)}}}{2i\pi\hbar(t-t_c)/m} \frac{e^{i\frac{m[(y_1-y_0)^2+(z_1-z_0)^2]}{2\hbar(t-t_c)}}}{2i\pi\hbar(t-t_c)/m} \ . \tag{94}$$

Then, to get the interference pattern on the screen, we have to compute the square modulus of the N-slit propagator:

$$I^{(N)}_{\rm Trunc}(\mathbf{r}, t; \mathbf{r}_0, 0|\mathbf{r}_1, t_c) \equiv I_0 \times |K^{(N)}_{\rm Trunc}(\mathbf{r}, t; \mathbf{r}_0, 0|\mathbf{r}_1, t_c)|^2 \ . \tag{95}$$

Remark.: In [14], for a initial Gaussian wave packet in the limit $\sigma \to 0$ (σ is the width of the Gaussian), it is proved that the density of probability is proportional to the square of the propagator:

$$P^{(N=1)}(\mathbf{r}, t; \mathbf{r}_0, 0|\mathbf{r}_1, t_c) = \frac{\pi^2\hbar^2 t_c^2}{mab} \frac{2\pi\hbar t_c}{m} |K^{(N=1)}(\mathbf{r}, t; \mathbf{r}_0, 0|\mathbf{r}_1, t_c)|^2 = \frac{1}{4ab\gamma^3} |F_{t,t_c}(z, a)|^2 |F_{t,t_c}(y, b)|^2 \ , \tag{96}$$

where we generalized the probabilistic interpretation developed in [14] for a two dimensional slit, and where the factor $\frac{2\pi\hbar t_c}{m}$ in the second equality in (96) come from the Gaussian normalisation in the x-direction. Notice that by (94), we can extend the result for all N by recursion.

6.2 Appendix 2: Derivation of the one-point source propagator

By (29), the one-point source propagator is given by

$$K(\mathbf{r},t;\mathbf{r}_0,0|\mathbf{r}_1) \equiv \int_0^t d\tau \left[\frac{-x_0}{\tau}\eta_1 + \frac{x}{t-\tau}\eta_2\right] G_0(\mathbf{r}-\mathbf{r}_1,t-\tau)G_0(\mathbf{r}_1-\mathbf{r}_0,\tau) \tag{97}$$

$$= \eta_2 K^{(D)}(\mathbf{r},t;\mathbf{r}_0,0|\mathbf{r}_1) + \eta_1 K^{(N)}(\mathbf{r},t;\mathbf{r}_0,0|\mathbf{r}_1) \tag{98}$$

where we have introduced the Dirichlet part:

$$K^{(D)}(\mathbf{r},t;\mathbf{r}_0,0|\mathbf{r}_1) = \int_0^t d\tau \left[\frac{x}{t-\tau}\right] G_0(\mathbf{r}-\mathbf{r}_1,t-\tau)G_0(\mathbf{r}_1-\mathbf{r}_0,\tau) \tag{99}$$

and the Neumann part:

$$K^{(N)}(\mathbf{r},t;\mathbf{r}_0,0|\mathbf{r}_1) = \int_0^t d\tau \left[\frac{-x_0}{\tau}\right] G_0(\mathbf{r}-\mathbf{r}_1,t-\tau)G_0(\mathbf{r}_1-\mathbf{r}_0,\tau) \tag{100}$$

We will use the Laplace transform defined by

$$LT\left[f(\tau);\tau,s\right] = \int_0^{+\infty} d\tau\ e^{-s\tau} f(\tau)$$

and the inverse Laplace transform

$$LT^{-1}\left[F(s);s,\tau\right] = \int_{c-i\infty}^{c+i\infty} \frac{ds}{2i\pi}\ e^{\tau s} F(s),$$

where c is a real-valued constant chosen such that the integral remains finite. We have the following Laplace transforms (see equations (28) P.147 §4.5 and (5) P.246 §5.6 in [31]):

$$LT\left[\left(\frac{m}{2i\pi\hbar t}\right)^{3/2} e^{i\frac{m|\mathbf{r}|^2}{2\hbar t}};t,s\right] = \frac{e^{i|\mathbf{r}|\sqrt{2mis/\hbar}}}{2i\pi\hbar|\mathbf{r}|/m} \tag{101}$$

$$LT\left[\frac{1}{t}\left(\frac{m}{2i\pi\hbar t}\right)^{3/2} e^{i\frac{m|\mathbf{r}|^2}{2\hbar t}};t,s\right] = \frac{e^{i|\mathbf{r}|\sqrt{2mis/\hbar}}}{2i\pi|\mathbf{r}|^2}\left(-\sqrt{2mis/\hbar}+\frac{i}{|\mathbf{r}|}\right) \tag{102}$$

So by (100) and (101) we get

$$K^{(N)}(\mathbf{r},t;\mathbf{r}_0,0|\mathbf{r}_1)$$
$$=\frac{-mx_0}{\hbar}\times LT^{-1}\left[\frac{e^{i|\mathbf{r}-\mathbf{r}_1|\sqrt{2mis/\hbar}}}{2i\pi|\mathbf{r}-\mathbf{r}_1|}\frac{e^{i|\mathbf{r}_1-\mathbf{r}_0|\sqrt{2mis/\hbar}}}{2i\pi|\mathbf{r}_1-\mathbf{r}_0|^2}\left(-\sqrt{2mis/\hbar}+\frac{i}{|\mathbf{r}_1-\mathbf{r}_0|}\right);s,t\right] \tag{103}$$

putting $\mathbf{u}_1=\mathbf{r}_1-\mathbf{r}_0$, $\mathbf{u}_2=\mathbf{r}-\mathbf{r}_1$, (103) is equal to

$$\frac{-mx_0}{\hbar}\frac{(|\mathbf{u}_2|+|\mathbf{u}_1|)^2}{|\mathbf{u}_2||\mathbf{u}_1|^2}\times$$
$$LT^{-1}\left[\frac{e^{i(|\mathbf{u}_2|+|\mathbf{u}_1|)\sqrt{2mis/\hbar}}}{(2i\pi|\mathbf{u}_2|+|\mathbf{u}_1|)^2}\left(-\sqrt{2mis/\hbar}+\frac{i}{|\mathbf{u}_2|+|\mathbf{u}_1|}+\left(\frac{i}{|\mathbf{u}_1|}-\frac{i}{|\mathbf{u}_2|+|\mathbf{u}_1|}\right)\right);s,t\right] \tag{104}$$

then using the inversion formulas (101), we get:

$$K^{(N)}(\mathbf{r},t;\mathbf{r}_0,0|\mathbf{r}_1)=A_t^{(N)}(\mathbf{r},\mathbf{r}_0|\mathbf{r}_1)e^{i\varphi(\mathbf{r},\mathbf{r}_0|\mathbf{r}_1)} \tag{105}$$

where the amplitude is given by:

$$A_t^{(N)}(\mathbf{r},\mathbf{r}_0|\mathbf{r}_1)=\frac{-x_0}{(2i\pi\hbar t/m)^{3/2}}\left(\frac{m}{2i\pi\hbar t}\frac{(|\mathbf{r}-\mathbf{r}_1|+|\mathbf{r}_1-\mathbf{r}_0|)^2}{|\mathbf{r}-\mathbf{r}_1||\mathbf{r}_1-\mathbf{r}_0|^2}+\frac{1}{2\pi|\mathbf{r}_1-\mathbf{r}_0|^3}\right) \tag{106}$$

and the phase by:

$$\varphi_t(\mathbf{r},\mathbf{r}_0|\mathbf{r}_1)\equiv\frac{m}{2\hbar t}(|\mathbf{r}-\mathbf{r}_1|+|\mathbf{r}_1-\mathbf{r}_0|)^2 \tag{107}$$

Similary for the Dirichlet boundary condition, by the symmetries $t_1\leftrightarrow t-t_1$ and $u_1\leftrightarrow u_2$ in (103), we get that the amplitude is given by:

$$A_t^{(D)}(\mathbf{r},\mathbf{r}_0|\mathbf{r}_1)=\frac{x}{(2i\pi\hbar t/m)^{3/2}}\left(\frac{m}{2i\pi\hbar t}\frac{(|\mathbf{r}-\mathbf{r}_1|+|\mathbf{r}_1-\mathbf{r}_0|)^2}{|\mathbf{r}-\mathbf{r}_1|^2|\mathbf{r}_1-\mathbf{r}_0|}+\frac{1}{2\pi|\mathbf{r}-\mathbf{r}_1|^3}\right) \tag{108}$$

and that the phase does not change and is given by (107).

6.3 Appendix 3: Diffraction patterns

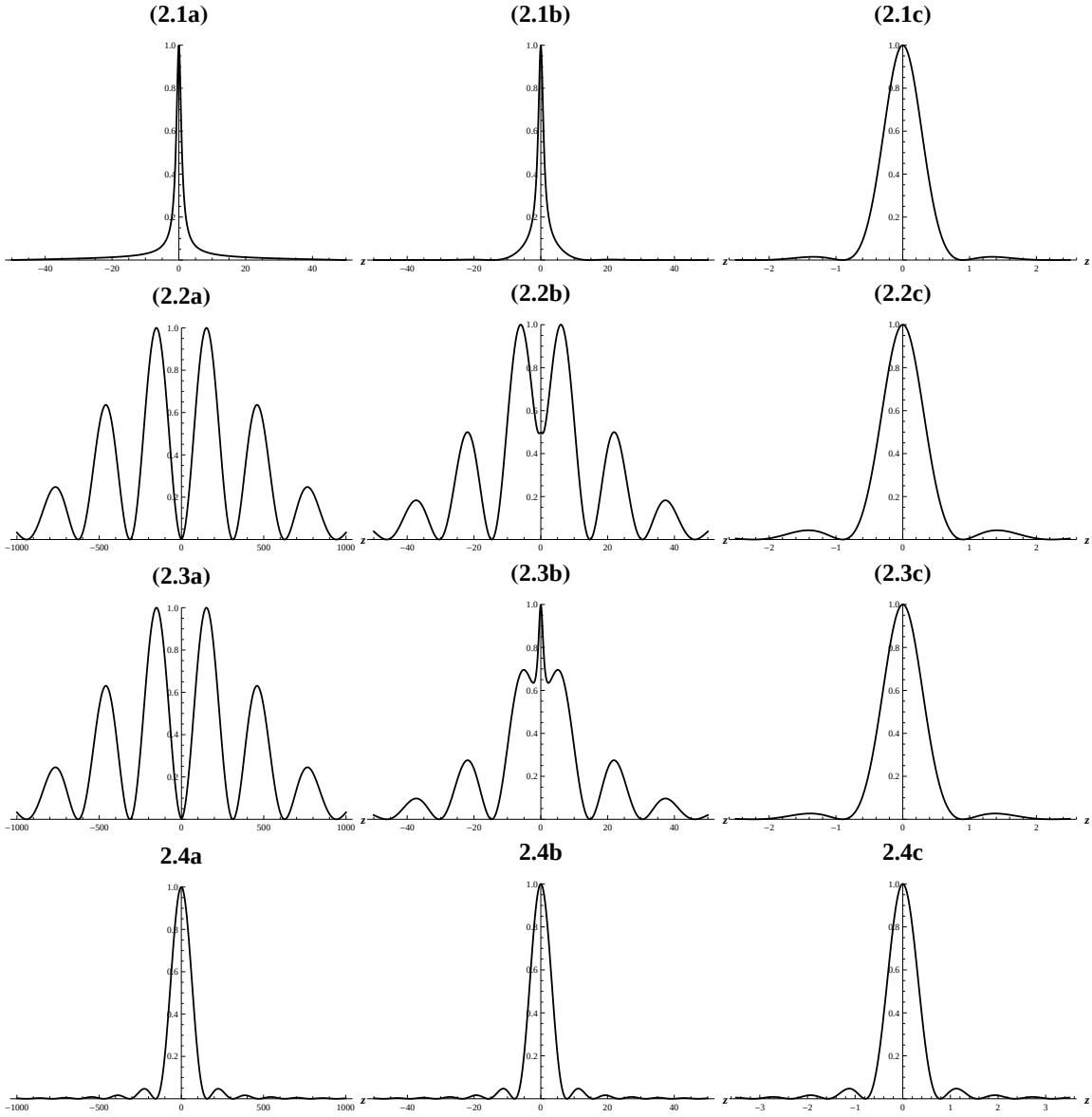

Figure 2: Semi-classical transition for the single-slit interference pattern. We take $x = 1,\ x_1 = 0,\ x_0 = -1$, $a = 0.01$ and $b = 0.1$ in the units $\hbar = m = 1$. We represent the relative populations computed as the square modulus of the propagators (28) respectively for the Dirichlet (Fig.2.1a-2.1c), Newmann (Fig.2.2a-2.2c) and free (Fig.2.3a-2.3c) boundary conditions and also for the truncation approximation (Fig.2.4a-2.4c) by the Equation (93), with $t = 1$ for the figures at the left (a), $t = 0.05$ at the middle (b) and $t = 0.005$ at the right (c).

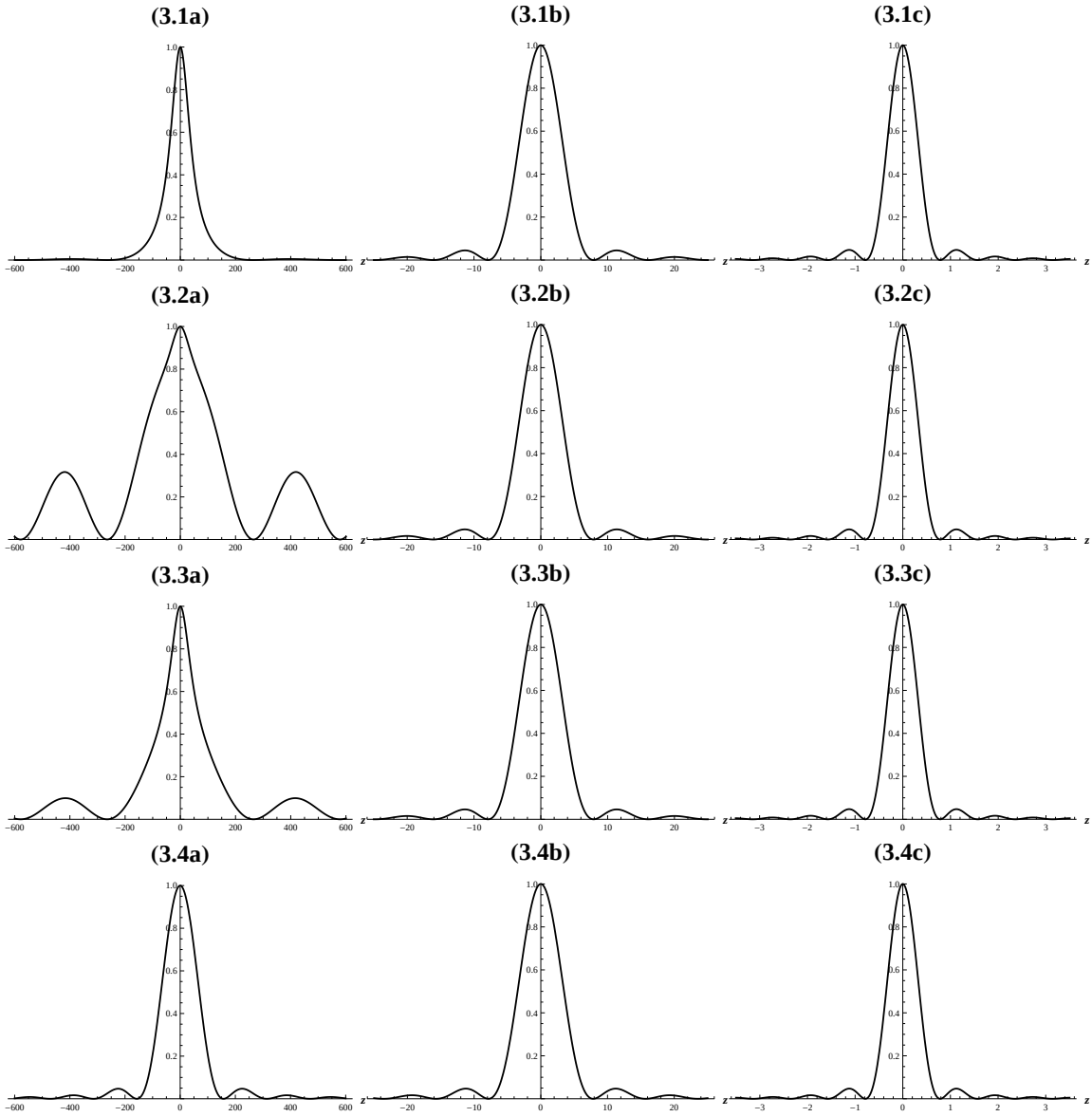

Figure 3: Truncation approximations for the single-slit interference pattern. We take $x = 50,\ x_1 = 0,\ x_0 = -50,\ a = 0.01$ and $b = 0.1$ in the units $\hbar = m = 1$. We represent the relative populations computed as the square modulus of the propagators (28) respectively for the Dirichlet (Fig.3.1a-3.1c), Newmann (Fig.3.2a-3.2c) and free (Fig.3.3a-3.3c) boundary conditions and also for the truncation approximation (Fig.3.4a-3.4c) by the Equation (93), with $t = 1$ for the figures at the left (a), $t = 0.05$ at the middle (b) and $t = 0.005$ at the right (c).

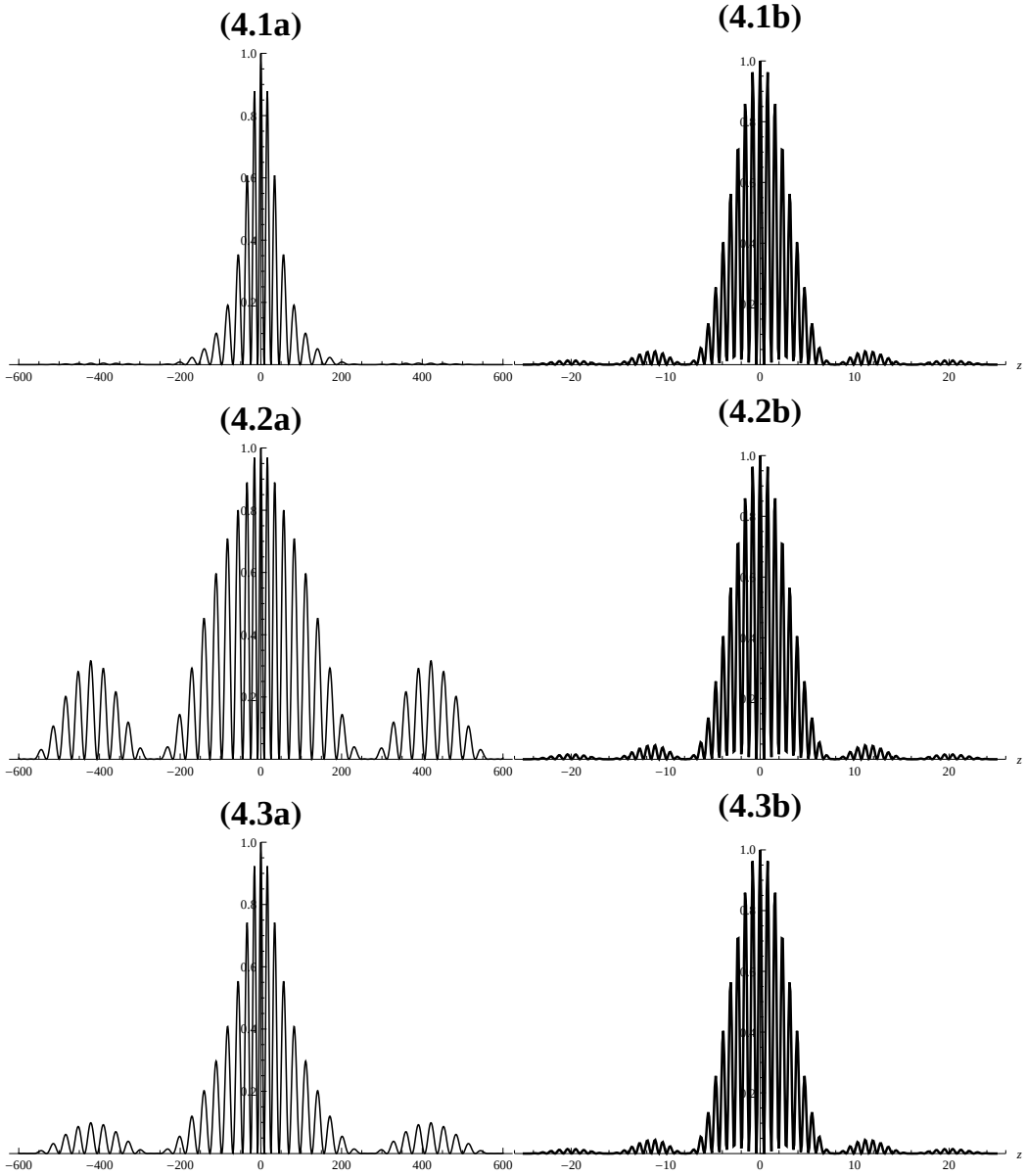

Figure 4: Double-slit interference patterns. We take $x = 50,\ x_1 = 0,\ x_0 = -50,\ a = 0.01,\ b = 0.1$ and $d = 0.1$, in the units $\hbar = m = 1$. We represent the relative populations computed as the square modulus of the propagators (77) respectively for the Dirichlet (Fig.4.1a-4.1b), Newmann (Fig.4.2a-4.2b) and free (Fig.4.3a-4.3b) boundary conditions with $t = 1$ for the figures at the left (a), $t = 0.05$ at the right (b).

References

[1] C. Jönsson, "Elektroneninterferenzen an mehreren künstlich hergestellten Feinspalten", Z. Phys. **161** (4), 454-474 (1961).

[2] C. Jönsson, "Electron Diffraction at Multiple Slits", Am. J. Phys. **42**(1), 4-11 (1974).

[3] O. Donati, G. F. Missiroli, G. Pozzi, "An Experiment on Electron Interference", Am. J. Phys. **41**, 639-644 (1973).

[4] P. G. Merli, G. F. Missiroli, G. Pozzi, "On the statistical aspect of electron interference phenomena", Am. J. Phys. **44**(3), 306-307 (1976).

[5] A. Tonomura, J. Endo, H. Ezawa, T. Matsuda and T. Kawasaki, "Demonstration of single-electron buildup of an interference pattern", Am. J. Phys. **57**(2), 117-120 (1989).

[6] R. P. Feynman, R. B. Leighton, and M. L. Sands , *The Feynman Lectures on Physics* (Addison-Wesley, Reading, MA, 1965).

[7] R. Bach, D. Pope, S. -H. Liou, H. Batelaan, "Controlled double-slit electron diffraction", New J. Phys. **15**, 033018 (2013).

[8] S. Frabboni, C. Frigeri, G. C. Gazzadi, G. Pozzi, "Two and three slit electron interference and diffraction experiments", Am. J. Phys. **79** (6), 615-618 (2011).

[9] A. Zeilinger, R. Gähler, C. G. Shull, W. Treimer, W. Mampe, "Single- and double-slit diffraction of neutrons", Rev. Mod. Phys. **60**(4), 1067-73 (1988).

[10] F. Shimizu, K. Shimizu, H. Takuma, "Double-slit interference with ultracold metastable neon atoms", Phys. Rev. A. **46**(1), R17-R20 (1992).

[11] O. Nairz, M. Arndt, A. Zeilinger, "Quantum interference experiments with larges molecules", Am. J. Phys. **71**(4), 319-325 (2003).

[12] R. P. Feynman and A. R. Hibbs, *Quantum Mechanics and Path Integrals* (New York: McGraw-Hill), 3rd. ed. (1965).

[13] A. O. Barut, S. Basri, "Path integrals and quantum interference", Am. J. Phys. **60**(10), 896-899 (1992).

[14] M. Beau, "Feynman path integral and electron diffraction slit experiments" Eur. Journ. Phys. **33**(15), 1023-1039 (2012).

[15] A. Zecca, "Two-Slit Diffraction Pattern for Gaussian Wave Packets", Int. J. Theo. Phys. **38**(3), 911-918 (1999).

[16] M. Moshinsky, "Diffraction in Time", Phys. Rev. **88**(3), 625-631 (1952).

[17] P. Szriftgiser, D. Guéry-Odelin, M. Arndt, J. Dalibard, "Atomic Wave Diffraction and Interference Using Temporal Slits", Phys. Rev. Lett. **77**(1), 4-7 (1996).

[18] C. Brukner, A. Zeilinger, "Diffraction of matter waves in space and in time", Phys. Rev. A. **56**(5), 3804-3824 (1997).

[19] P. M. Morse and H. Feshbach, *Methods of Theoretical Physics*, (McGraw-Hill, New York, 1953).

[20] A. Goussev, "Huygens-Fresnel-Kirchhoff construction for the quantum propagator with application to diffraction in space and time" Phys. Rev. A. **85**(1), 013626-013636 (2012).

[21] A. Goussev, "Time diffraction: an exact model" Phys. Rev. A. **87**(5), 053621 (2013).

[22] A. del Campo and J. G. Muga, "Single-particle matter wave pulses", J. Phys. A: Math. Gen. **38**(45), 9803-9819 (2005)

[23] A. del Campo, J. G. Muga, and M. Moshinsky, "Time modulation of atom sources", J. Phys. B: At. Mol. Opt. Phys. **40**, 975 (2007).

[24] A. del Campo, G. García-Calderón, J.G. Mugad, "Quantum transients", Phys. Rep. **476**(1)-(3), 1-50 (2009).

[25] G. Kälbermann, "Single- and double-slit scattering of wavepackets", J. Phys. A: Math. Gen. **35**(21), 4599-4616 (2002).

[26] G. Kälbermann, "Diffraction of wave packets in space and time", J. Phys. A: Math. Gen. **34**(33), 6465-6480 (2001).

[27] G. Kälbermann, "Wave packet diffraction in the KronigPenney model", J. Phys. A: Math. Gen. **35**(4), 1045-1053 (2002).

[28] M. Gondran, A. Gondran, "Numerical simulation of the double slit interference with ultracold atoms", Am. J. Phys. **73**(6), 507-515 (2005).

[29] M. Abramowitz and I. A. Stegun, *Handbook of Mathematical Functions*, (Dover, New York, 1965).

[30] M. Born and E. Wolf, *Principles of Optics: Electromagnetic Theory of Propagation, Interference and Diffraction of Light*, 4th ed. (Pergamon, Oxford, 1969).

[31] A. Erdelyi, *Tables of Integral Transforms, Vol. 1* (McGraw-Hill Inc. US, 1954).